Office of Satellite and Product Operations

Environmental Satellite Processing Center

Enterprise Active Fire System Algorithm Theoretical Basis Document

Version 1.3

August 11, 2023

Prepared by: Earth Resources Technology, Inc.

U.S. Department of Commerce
National Oceanic and Atmospheric Administration
National Environmental Satellite, Data, and Information Service
Office of Satellite and Product Operations

Changes/Revisions Record

This algorithm theoretical basis document is changed as required to reflect system, operational, or organizational changes. Modifications made to this document are recorded in the Changes/Revisions Record below. This record will be maintained throughout the life of the document.

Version Number	Date	Description of Change/Revision	Section/Pages Affected	Changes Made by Name/Title/ Organization
1.2	12/5/2022	New ATBD Document according to NOAA /NESDIS/STAR Document Guideline		Wei Guo (IMSG)
1.3	08/11/2023	Cover page, Changes/Revisions Record, and Preface added to EFIRE ATBD Version 1.2	Cover page, Changes/Revisions Record, Preface	Hannah Willett, Technical Writer, ERT Inc.
1.3	08/15/2023	Quality Assurance	Cover page, Changes/Revisions Record, Preface	Clint Sherwood, Quality Assurance Manager, ERT Inc.

Preface

This document comprises the National Oceanic and Atmospheric Administration (NOAA) National Environmental Satellite, Data, and Information Service (NESDIS), Office of Satellite and Product Operations (OSPO), publication of this Enterprise Active Fire System (EFIRE) Algorithm Theoretical Basis Document. This document reflects current operations for the DOC/NOAA/NESDIS Environmental Satellite Processing Center (ESPC) (NOAA5045) information technology systems. This document describes the established ESPC procedure for users of EFIRE in accordance with Federal, DOC, NOAA, NESDIS and OSPO requirements.

NOAA/NESDIS/OSPO acknowledges the efforts of ERT Inc. personnel for their preparation of this document. Future updates and revisions to this document will be produced and controlled by DOC/NOAA/NESDIS for ESPC information technology systems.

The published version of this document can be found at the OSPO SharePoint Products Library.

Table of CONTENT

Contents

List of Tables

List of Figures

LIST OF ACRONYMS

ABI	Advanced Baseline Imager
AIT	Algorithm Integration Team
ASCII	American Standard Code for Information Interchange
ASTER	Advanced Spaceborne Thermal Emission and Reflection Radiometer
ATBD	Algorithm Theoretical Base Document
AVHRR	Advanced Very High Resolution Radiometer
AWG	Algorithm Working Group
CDR	Critical Design Review
CFCLD	Constant Fire with CLouDs
CFNOCLD	Constant Fire with NO CLouDs
CIMSS	Cooperative Institute for Meteorological Satellite Studies
CIRA	Cooperative Institute for Research in the Atmosphere
CM	Configuration Management
CMMI	Capability Maturity Model Integration
CONUS	CONterminous United States
CPU	Central Processing Unit
CREST	Cooperative Remote Sensing and Technology Center
DG	Document Guideline
EFIRE	Enterprise Fire detection system
EPL	Enterprise Product Lifecycle
ETM+	Enhanced Thematic Mapper Plus
FD	Full Disk
FOV	Field Of View
FRE	Fire Radiative Energy
FRP	Fire Radiative Power
FRP_{DEF}	Fire Radiative Power DEFinition
FRP_{MIR}	Fire Radiative Power Middle InfraRed
GLCC	Global Land Cover Characteristics
GOES	Geostationary Operational Environmental Satellite
GS-F&PS	Ground Segment Functional and Performance Specification
IGFOV	Instantaneous Ground Field Of View
IPT	Integrated Product Team
IR	Infrared
JAMI	Japanese Advanced Meteorological Imager
K	Kelvin
LDCM	Landsat Data Continuity Mission
N/A	Not Applicable
NASA	National Aeronautics and Space Administration

NEdT	Noise Equivalent delta Temperature
NCEP	National Center for Environmental Prediction
NESDIS	National Environmental Satellite, Data, and Information Service

NOAA	National Oceanic and Atmospheric Administration
NPOESS	National Polar-orbiting Operational Environmental Satellite System
MET	short for METeosat
METimage	The EUMETSAT Polar System-Second Generation (EPS-SG) Visible Infrared Imager (VII)
MIR	Middle InfraRed
MODIS	Moderate Resolution Imaging Spectroradiometer
MSG	Meteosat Second Generation
MTSAT	Multifunctional Transport Satellite
MRD	Mission Requirement Document
NCEP	National Center for Environmental Prediction
NetCDF4	Network Common Data Form 4
OCD	Operations Concept Document
OLI	Operational Land Imager
PAL	Process Asset Library
PDR	Preliminary Design Review
PM	Particulate Matter
PRR	Project Requirements Review
PSF	Point Spread Function
QA	Quality Assurance
QC	Quality Control
RAD	Requirements Allocation Document
RAS	Requirements Allocation Sheet
RHTM	Requirements Horizontal Traceability Matrix
RNM	Requirements/Needs Matrix
RPP	Research Project Plan
RVTM	Requirements Vertical Traceability Matrix
SEVIRI	Spinning Enhanced Visible and InfraRed Imager
SPSRB	Satellite Products and Services Review Board
SRR	System Readiness Review
SSEC	Space Science and Engineering Center
STAR	Center for Satellite Applications and Research
SWA	Software Architecture Document
TBD	To Be Determined
TD	Training Document
TPW	Total Precipitable Water
UMD	University of MarylanD
UTC	Coordinated Universal Time
UW	University of Wisconsin
UW BF	University of Wisconsin Baseline Fit
VAS	Visible Infrared Spin Scan Radiometer (VISSR) Atmospheric Sounder

VFCLD	Variable Fire with CLouDs
VFNOCLD	Variable Fire NO CLouDs
VIIRS	Visible Infrared Imaging Radiometer Suite
VII	Visible Infrared Imager
VVP	Verification and Validation Plan
WF_ABBA	Wild Fire Automated Biomass Burning Algorithm

ABSTRACT

The Enterprise Active Fire system (EFIRE) is an integrated system to detect active fires/hot spots by using multiple satellite sensors. It adopts the fire detection algorithms currently used in NOAA operational active fire detection systems, checks for known persistent anomalies such as oil/gas, volcanoes and solar farms and generates fire products in a common format. The output includes fire pixel locations, fire characteristics, and other metadata fields.

EFIRE system performs fire detection by using data from sensors below:

- The Advanced Baseline Imager (ABI) on Geostationary Operational Environmental Satellite (GOES),
- The Visible Infrared Imaging Radiometer Suite (VIIRS) on the Suomi NPP, NOAA-20 (JPSS-1) and NOAA-21 (JPSS-2) satellites,
- The Spinning Enhanced Visible and InfraRed Imager (SEVIRI) on the Meteosat Second Generation (*MSG*) satellites,
- The future EUMETSAT Polar System-Second Generation (EPS-SG) Visible Infrared Imager (VII) (METimage)

The Enterprise Active Fire system algorithm theoretical basis document (ATBD) provides high level description of diurnal fire detection, monitoring, and characterization utilizing above sensors. The purpose of this ATBD is to provide fire product developers, reviewers and users with a high level scientific and mathematical description of the EFIRE system. The underlying fire detection algorithm includes 1) The GOES Wildfire Automated Biomass Burning Algorithm (WF_ABBA) that has been running operationally in NESDIS since 2002, 2) the VIIRS MOD bands fire detection algorithm and 3) the VIIRS IMG bands fire detection algorithm. The VIIRS MOD bands fire detection algorithm was also tuned and applied to The EUMETSAT Polar System-Second Generation (EPS-SG) Visible Infrared Imager (VII) (METimage).

Although these sensor specific fire algorithms are obviously different in many ways, they share the same general concept. They are a dynamic multispectral thresholding contextual algorithm that is based on the sensitivity of the mid-wave infrared (MWIR) ~4μm band to high temperature sub-pixel anomalies relative to the less sensitive 11μm thermal infrared (TIR) window band. The algorithm uses the shortwave reflectance (0.64 μm) when available during the daytime to determine surface reflectivity for cloud identification. The algorithm incorporates statistical techniques to automatically identify hot spot pixels in the observed imagery.

Since these algorithms have already well documented, this ATBD will briefly discuss each algorithm and focus on improvement and other features of the EFIRE system. Please refer to the corresponding ATBDs for specific details of the algorithms.

1 INTRODUCTION

The purpose, users, scope, related documents and revision history of this document are briefly described in this section. Section 2 gives an overview of the observing system, products generated, and instrument characteristics. Section 3 describes the fire algorithms. Section 4 illustrates how to implement multiple fire detection algorithms in one system. Section 5 describes the output format of EFIRE product. Test cases are presented in Section 6. Practical considerations including numerical computation consideration; programming and procedural considerations, quality assessment and diagnostics; exception handling are discussed in Section 7. Section 8 shows the result of validating SEVIRI and ABI fire product by using Landsat data. Assumptions and limitations are presented in Section 9 and include discussion of performance, assumed sensor performance, and pre-planned product improvements. The last section provides a list of references.

1.1 Purpose of This Document

This document (ATBD) provides high level description of diurnal fire detection, monitoring, and characterization utilizing various sensor data. The purpose is to provide fire product developers, reviewers and users with a theoretical description (scientific and mathematical) of the fire detection and characterization algorithms. This document presents an overview of the requirements for the EFIRE product, sensor characteristics pertinent to fire monitoring, required input data, the physical and mathematical backgrounds of the fire algorithms, predicted performance based on case study analyses, practical considerations, and assumptions and limitations. Also, this document provides information useful to anyone maintaining or modifying the original algorithms.

1.2 Who Should Use This Document

The intended users of this document are those interested in understanding the physical basis of the EFIRE algorithm and how to use the output of this algorithm for a variety of fire applications. This includes a broad user community with various degrees of satellite expertise. The diurnal fire detection and characterization product is utilized by an interdisciplinary user community in fire weather applications, hazards monitoring/assessment, resource management, global change research, land-use/land-cover change analyses, fire dynamics research, emissions monitoring and modeling, air quality, and transportation.

1.3 Inside Each Section

This document is broken down into the following main sections.

- **Observing System Overview**: Provides relevant details of the sensors and provides a brief description of the products generated by the fire algorithm.
- **Algorithm Description**: Provides a brief description of the algorithm
- **EFIRE features**: illustrates how to implement multiple fire detection algorithms in one system

- **EFIRE output**: describes the output format of EFIRE product Test Data Sets and Outputs: Provides a description of the test data sets used to develop and implement the algorithm and characterize the performance of the algorithm. The result of comparing SEVIRI and ABI fire product against VIIRS fire product was presented.
- **Practical Considerations**: Provides a brief overview of the issues relating to numerical computation, programming and procedures, quality assessment and diagnostics, exception handling, and algorithm validation.
- **Assumptions and Limitations**: Provides an overview of the current limitations of the instrument and algorithm and possible avenues for addressing some of these limitations with further algorithm development.
- **Validation**: provides the result of validating SEVIRI and ABI fire product by using Landsat data

1.4 Related Documents

- ABI fire detection ATBD.
- VIIRS-M bands fire detection ATBD.
- VIIRS-I bands fire detection ATBD.

Other related references are listed in the Reference Section.

1.5 Revision History

Version 1.2: Created by Wei Guo (IMSG), its intent was to accompany the delivery of the version 1.2 algorithm to the Algorithm Scientific Software. Integration and System Transition Team (ASSISTT)**.**

Table 1-1 Version History

Version	Description	Revised Sections	Date
1.2	New ATBD Document according to NOAA /NESDIS/STAR Document Guideline		12/5/2022

2 OBSERVING SYSTEM OVERVIEW

Most meteorological satellites, including geostationary satellites and polar orbiting satellites, provide remote sensing observations in MWIR (~4μm) and TIR (~11μm) bands. The 4μm band is sensitive to high temperatures on the surface. Fire signals can be detected by using the difference of brightness temperature (BT) at 4μm and 11μm, also utilizing the contrast between the BT of these channels and surrounding background pixels. Actual wavelengths of these bands may vary by sensor (for example, 3.9um for ABI band 7, and 3.97 - 4.13 μm for VIIRS band M13). Data of other bands are also used for cloud test and false alarm rejection.

Several fire detection algorithms have been developed during the last two decades. They were further integrated into one system: enterprise active fire detection system (EFIRE system).

This section summarizes the sensors on various satellite observing systems used by EFIRE system.

2.1 Sensors /satellites used by EFIRE

EFIRE system performs fire detection using data observed by the various sensors/ satellites, including:

- **VIIRS**: The Visible Infrared Imaging Radiometer Suite (VIIRS) on the Joint Polar Satellite System (JPSS),
- **ABI**: The Advanced Baseline Imager (ABI) on the Geostationary Environmental Operational Satellite (GOES) -R series
- **SEVIRI**: The Spinning Enhanced Visible and InfraRed Imager (*SEVIRI*) on EUMESAT Meteosat Second Generation (MSG) satellites.
- **VII (**Visible and Infrared Imager, **METimage)**: It is possible to extend the system to other sensors, such as METImage measurements onboard EUMETSAT's upcoming MetOp-Second Generation polar missions.

Table 2-1 sensors / satellites used for fire detection

Sensor	Satellite	Domain
ABI	G16, G17, G18	RADF,RADC,RADM1,RADM2
VIIRS	SNPP, NOAA-20 (J01), NOAA-21 (J02)	MOD, IMG granule
SEVIRI	Meteosat 8, 9,11 (MSG1,MSG2, MSG4)	FD
VII (METimage)	SGA1	granule

Table 2-2 lists the names of bands used for fire detection by sensors.

Table 2-2 Bands used for fire detection

	ABI	VIIRS-M	VIIRS-I	SEVIRI	METimage	Remark
VIS	ABI_Band02	SVM05	SVI01	VIS006	vii_668	
NIR	ABI_Band03	SVM07	SVI02	VIS008	vii_865	

2 µm Reflectance	ABI_Band06	SVM11	SVI03	IR_016	vii_2250	
3.9 µm BT	ABI_Band07	SVM13	SVI04 SVM13	IR_039	vii_3959	
10 µm BT	ABI_Band13			IR_097		optional
11 µm BT	ABI_Band14	SVM15	SVI05	IR_108	vii_10690	
12 µm BT	ABI_Band15	SVM16		IR_120	vii_12020	optional
			IVCDB			VIIRS dual-gain unaggregated radiances
Geometry		GMTCO	GITCO			VIIRS geolocation

2.2 ABI data for fire detection

ABI radiance data are provided in four domains: full disk, CONUS/PACUS (Conterminous US / Pacific US) and two mesoscale regions. The observation frequency also varies by domain.

The ABI radiance bands used by the EFIRE system were listed in below tables. The resolutions of ABI radiances for VIS, NIR and IR bands are different, re-mapping high resolution image to the resolution of IR band are required.

Table 2-3 Array size of ABI bands for fire detection

ABI Band	Wavelength (µm)	Array size (RADC)	Array size (RADF)	Array size (RADM1/RADM2)
2	0.64	10000 x 6000	21696 x 21696	2000 x 2000
3	0.87	5000 x 3000	10848 x 10848	1000 x 1000
6	2.25	2500 x 1500	5424 x 5424	500 x 500
7	3.89	2500 x 1500	5424 x 5424	500 x 500
13	10.0	2500 x 1500	5424 x 5424	500 x 500
14	11.19	2500 x 1500	5424 x 5424	500 x 500
15	12.27	2500 x 1500	5424 x 5424	500 x 500

Table 2-4 Frequency of ABI observations in the current default operational mode (Mode 6)

	Image interval minutes	Resolution (3.9um band) km
RADF	10	2
RADC	5	2
RADM1	1	2
RADM2	1	2

2.3 VIIRS data for fire detection

The VIIRS instruments are available on the Suomi National Polar-orbiting Partnership (SNPP), NOAA-20 and NOAA-21 platforms and on future satellites of the Joint Polar Satellite System (JPSS). SNPP, NOAA-20 and NOAA-21 were launched on October 28, 2011, November 18, 2017, and November 10, 2022, respectively. They are in sun synchronous orbits with a 1:30pm ascending-node orbit at an altitude of 829 km; the primary and secondary operational missions are separated by 50 minutes (i.e. half of an Earth orbit).

The VIIRS instrument is a whiskbroom scanning radiometer with a swath width of 3060 km, providing full daily coverage both in the day and night side of the Earth. It has 22 spectral bands covering the spectrum between 0.412 μm and 12.01 μm, including 16 moderate resolution bands (M-bands) with a spatial resolution of 750 m at nadir, 5 imaging resolution bands (I-bands) – with a spatial resolution of 375 m at nadir, and one panchromatic DNB with a 750 m spatial resolution throughout the scan. Further details can be found in the VIIRS Sensor Data Record (SDR) User's Guide (NOAA Technical Report NESDIS 142A).

Two fire detection algorithms (VIIRS-M and VIIRS-I) were adopted in EFIRE system. The table below lists the VIIRS bands related to fire detection.

Table 2-5 VIIRS bands used by the fire detection and characterization algorithms

Band	Reflected Range (μm)	Resolution (m)	Band Explanation	Bands used by VIIRS-M Fire	Bands used by VIIRS-I Fire
I1	0.6 - 0.68	375	Near Infrared		X
I2	0.85 - 0.88	375	Shortwave Infrared		X
I3	1.58 - 1.64	375	Medium-wave Infrared		X
I4	3.55 - 3.93	375	Longwave Infrared		X
I5	10.5 - 12.4	375	Visible/Reflective		X
M5	0.662 - 0.682	750	Near Infrared	X	
M7	0.846 - 0.885	750	Shortwave Infrared	X	
M11	2.23 - 2.28	750	Medium-wave Infrared	X	
M13	3.97 - 4.13	750	Longwave Infrared	X	X
M15	10.26 - 11.26	750	Longwave Infrared	X	
M16	11.54 – 12.49	750	Longwave Infrared	X	

2.4 SEVIRI data for fire detection

The Spinning Enhanced Visible and InfraRed Imager (SEVIRI) is the imaging instrument on EUMESAT Meteosat Second Generation satellites and has the capacity to observe the Earth in 12

spectral channels. 11 of the channels are observation with full disk in resolution of 3km. Table 2-6 lists the bands used by EFIRE system, they are very close to the ABI bands for fire detection algorithm.

Table 2-6 SEVIRI bands for fire detection and characterization

Band	Wavelength (μm)	Resolution (m)
Band VIS 0.6 (VIS)	0.56 to 0.71	3000
Band VIS 0.8 (VIS)	0.74 to 0.88	3000
Band IR 1.6 (SWIR)	1.5 to 1.78	3000
Band IR 3.9 (MWIR)	3.48 to 4.36	3000
Band IR 9.7 (TIR)	9.38 to 9.94	3000
Band IR 10.8 (TIR)	9.8 to 11.8	3000
Band IR 12.0 (TIR)	11 to 13	3000

2.5 Products Generated

EFIRE generates fire products for each sensor (ABI, SEVIRI, VIIRS and VII) and satellite respectively and processes by each granule (or image). The main fire product is a NETCDF file, additional ASCII file is also created for quick access for the fire pixels.

Fire product in NETCDF file includes common output for fires such as:

Fire mask: 2D array as the same size as the input MWIR band, indicates classification the feature of each pixel; if it is classified as fire, records the fire class.

Quality flag: 2D array indicate the quality of fire retrieval for each pixel.

1D arrays of fire Pixels: records the values of major variables for fire pixels.

EFIRE output data format will be discussed in chapter 5.

3 Algorithm basics and implementation options integrated into the Enterprise Fire System

The EFIRE system incorporates processing logic from three existing NOAA operational fire detection algorithms. All three algorithms are based on a common logical framework that includes the interpretation of the following three basic signals:

1. Radiometric signal: distinct emitted signal from pixels that contain fires. This set of tests is based on fundamental laws of physics, in particular Planck's function and Wien's displacement law, which determine the absolute strength of the signal at a given wavelength.

2. Spatial heterogeneity: distinct signal from a pixel that contains active burning compared to neighboring "background" pixels.

3. Temporal persistence (geostationary only): persistent signal from subsequent observations to enhance detection confidence.

4. Additional tests and procedures to remove presumed false detections from hot and bright surfaces; flag cloudy pixels etc.

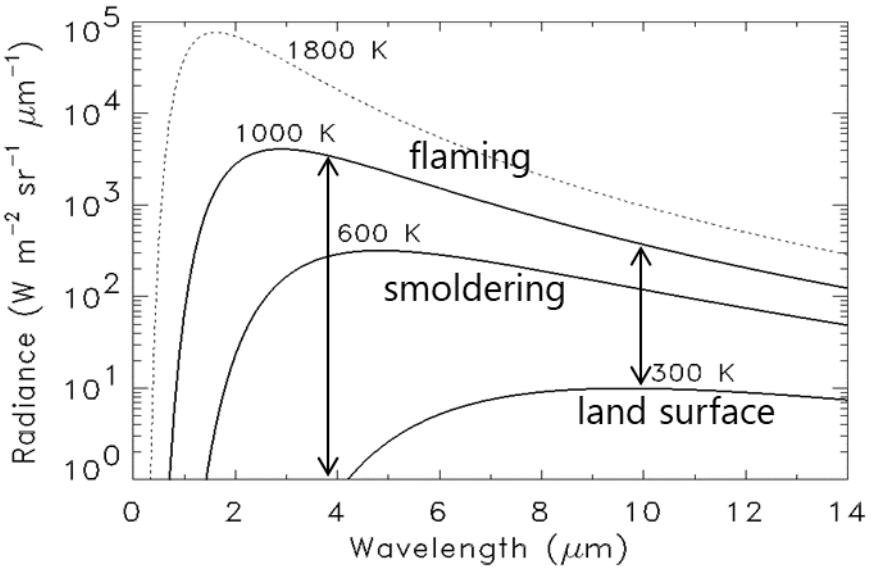

Figure 3-1 Variation of spectral radiance as a function of temperature as described by Planck's Law. Typical temperatures for flaming, smoldering and fire-free background are shown. Plot courtesy of Louis Giglio, University of Maryland.

Fire radiative power (FRP) in EFIRE is calculated by the method of Wooster *et al*. [2003, 2005] to derive FRP in Megawatts using the following equation:

$$FRP = \frac{S_p \cdot \sigma \cdot (L_F - L_B)}{c} \cdot 10^{-6}$$

Where L_F and L_B are the top-of-atmosphere fire pixel and background radiances ($W.m^{-2}.sr^{-1}.\mu m^{-1}$) on fire sensitive band of 3.9.µm, σ is the Stefan-Boltzmann constant (5.6704×10^{-8} $W.m^{-2}.K^{-4}$), S_p is the fire pixel area (m^2), and c is a constant (This depends on spectral response function of the fire sensitive band.)

The EFIRE system was developed based on several existing active fire detection algorithms (see list below).

WF_ABBA fire detection algorithm was converted from F90 to C++. It was adopted by EFIRE to process ABI and SEVIRI fire product. (ATBD: Schmidt et al., 2020)

VIIRS-VM (using VIIRS MOD bands only) fire detection was modified to use buffers with size of full granule. (ATBD: Giglio et al., 2020)

VIISR-I (using VIIRS IMG and MOD bands) fire detection algorithm was also modified to use simple big array (instead of many 2D arrays). (ATBD: Schroeder et al., 2020)

EFIRE output fire information in common output format. This greatly simplified the code structure and will be very helpful for end users of EFIRE products.

Table 3-1 Algorithms used by EFIRE system

Sensor	Resolution	Saturation	Orbit	Algorithm
JPSS VIIRS M-band	750m	high	1:30	VIIRS-VM (M-band)
JPSS VIIRS I-band	375m	low	1:30	VIIRS-I (Hybrid I/M band)
GOES-R ABI	2km	high	geo	WF-ABBA
Metop-SG/METimage*	1km	high	9:30	VII-VM
MSG/SEVIRI	3km	high	geo	SEVIRI-WF

* Metop-SG/METimage is not launched yet

4 EFIRE: Integrated Enterprise FIRE system

This chapter describes how to implement multiple fire detection algorithms in one system. Also introduces the shared modules.

4.1 Integrated existing fire detection algorithms into EFIRE system

Enterprise Fire Detection system was built by

- Converting WF_ABBA algorithm for ABI and SEVIRI from F90 to C++;
- Merging existing 2 VIIRS fire detection algorithms (VIIRS-I and VIIRS-M) into EFIRE C++ package;
- Introducing new structures to re-shape the code structure, make it easy to understand;
- Improving the algorithm by introducing additional data quality test on "sun glint pixels near the full disk edge", which removed a large number of obvious false alarms
- Using the common input/output interface (Class CNetFile) to easily access HDF4/ HDH5/ NETCDF files. This class (CNetFile) is a part of supporting library "gLib" which was developed by GuoW@imsg.com.
- Using one ancillary file ("EFIRE parameter file"), which includes all required ancillary data. These data came from more than 40 original files in various formats, including monthly emissivity, transmittance coefficients, land surface types (in NETCDF), persistent anomalies in GIS format), fire detection parameters, calibration parameters (in ASCII) and configure parameters et al.
- Using sharable variable names instead of sensor specific band names;
- Re-writing the algorithms as independent modules; this makes it possible to apply one algorithm to other sensors. For example,
    - It is optional to apply VIIRS-VM fire detection algorithm on ABI or SEVIRI data.
    - Apply fire VIIRS-VM category classification module to ABI and SEVIRI;
    - Mean and standard deviation of background BT was calculated as independent function
- Using the new method to manage the RAM: "ALLOCATE" function was used all the time so that the developer can be notified the name of file and function, and number of lines in the specific file if the exception occurs.
- Output Fire product in the same format for all sensors by using the new common data format.

4.2 Flow chart of EFIRE system

The flowchart below (Figure 4-1) shows the major modules of the EFIRE system.

When running in operational production system (operational mode), the only command line argument is the file name of process control file (PCF) file. It contains all input/output paths and satellite name. EFIRE will use the default algorithm for a given satellite.

The Input modules will read radiance files for specific senor (SEVIRI, ABI, VIIRS, METimage);

Ancillary data are read in from the single EFIRE parameter file. Then geometry angles (latitude, longitude, solar zenith and azimuth, satellite zenith and azimuth, gun glint angles are calculated in the ancillary module if they did not come with remote sensing data. Correction on reflectance field is also carried out.

Fire detection algorithms - Algorithm VM (tuned from VIIRS-M), Algorithm VIIRS-I and Algorithm WF (tuned from WF_ABBA) - were re-written as independent modules. Now it is optional to apply Algorithm VM to ABI or SEVIRI data.

EFIRE writes output NETCDF file by using a common output module, which makes possible generating fire products in the same format for a common set of basic variables. Optional variables may also be written into output NETCDF file. For example, the satellite parameters of GOES series satellites will be copied from radiance file, so that end user can use them to calculate the geolocation and geometry angles.

EFIRE also saves limited variables (including location, brightness temperature and FRP) to an ASCII file.

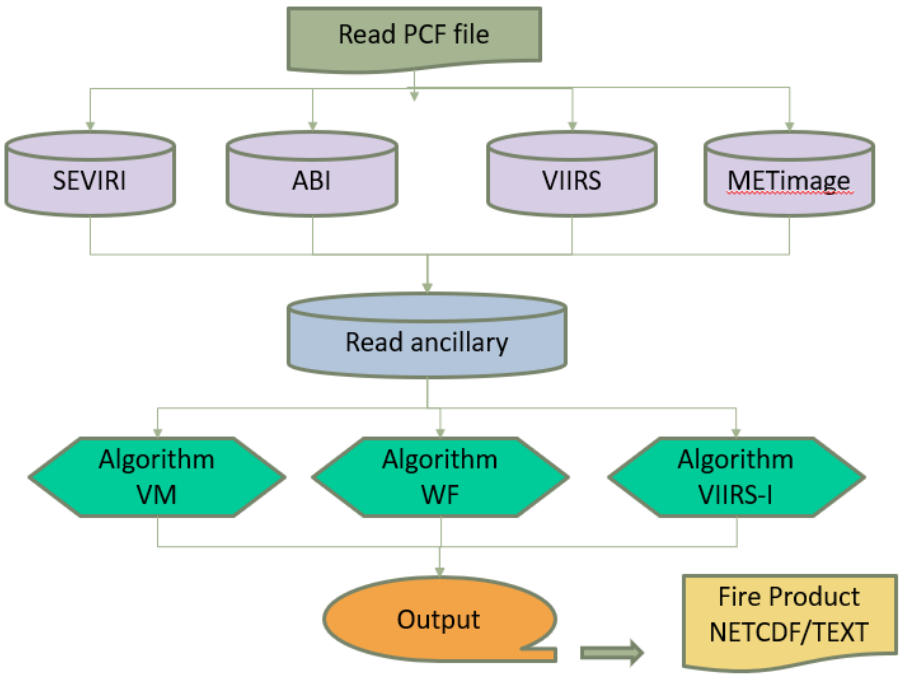

Figure 4-1 EFIRE data flow chart

4.3 Additional data quality test on sun glint near full disk image

One of the major improvements is that EFIRE system uses a new test on sun glint near the edge of ABI /SEVIRI full disk image.

It was found that a large number of obvious false alarm pixels near the edge of full disk image may be detected by the baseline WF_ABBA algorithm. Sometimes, this number can be as high as 10000 pixels per image. They appear as an arc shape along the edge of full disk and only occur when the sun-target-satellite is nearly on a straight line. It should be due to sun glint.

In the EFIRE system, pixel which satisfies the below test is considered as a sun glint pixel and will be treated as missing pixel.

$$(\theta v > 60 \;\&\&\; \theta g < 25) \;||\; \theta v > 70 \;\&\&\; \theta g < 30)$$

where, θv is the satellite zenith angle, and θg is sun glint angle

The false alarm was greatly reduced after applying above test.

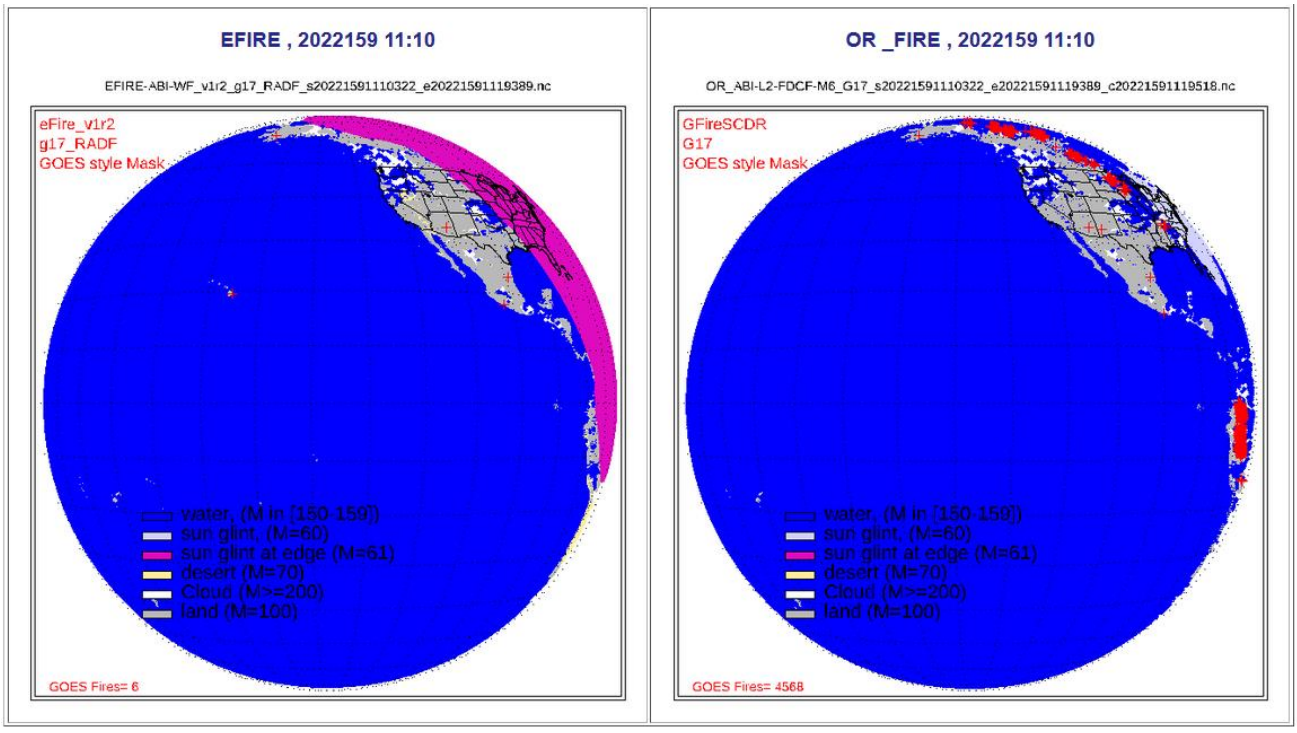

Figure 4-2 Fire mask images overlaid with fire pixels detected. (a) EFIRE product, (b) baseline WF_ABBA fire product.

4.4 List of shared modules of EFIRE system

Below is the list of shared modules of EFIRE system. They make sure EFIRE products are processed in the similar way for various sensors.

- Ancillary file:
- Metadata file for operator
- PCF file
- PSF file
- Fire category classification
- FRP calculation
- Geometry angles
- Persistent anomaly flags
- EFIRE Output files

4.5 Ancillary file

EFIRE used many static ancillary data, such as global surface types, land sea mask, persistent anomalies, list of volcanoes, legend of fire mask and QA flags, parameters for EFIRE algorithms etc. They were provided by a single "EFIRE parameter file".

Example file name: eFire_parameters_v1r2A.nc.

The content of the EFIRE parameter file came from 40+ original files in format of NETCDF, HDF4, text, csv and GIS shape files. When upgrading EFIRE software, only this file with corresponding version will be delivered to integration team. This helps to avoid the confusion if delivering multiple ancillary files with various versions.

Below lists the major content of the ancillary file. Please refer to the EFIRE Internal User Manual for more detailed description on each data field.

- Global 1km "Land Water",
- Global 1km "Surface Type",
- Global 1km "Ecosystem Type"
- Global 500m "Land Water" Mask
- Monthly Global Emissivity over land
- Persistent Anomalies
- Holocene Volcano list
- Parameters for fire detection algorithms
- FRP constant for each satellite
- Legends for fire mask and QA
- Radiance Transmittance Coefficients
- SEVIRI Calibration parameters
- Terrain Corrected Geolocation for ABI Full Disk Domain

4.6 Metadata file

A static metadata file (example: Static_Metadata.txt) is also required by EFIRE. The content of this file will be added to fire product as file attributes. It allows controlling static NETCDF file attributes without source code modifications.

4.7 PCF file

In operational mode, the EFIRE application will run under control of Process Control File. EFIRE PCF file provides all data paths and necessary parameters.

Table 4-1 Example of PCF file

```
INPUT_SEVIRI_BAND01 = ../data/L1b/MSG1/2021150/MSG1_IODC___-VIS006___-202105301200.nc
INPUT_SEVIRI_BAND02 = ../data/L1b/MSG1/2021150/MSG1_IODC___-VIS008___-202105301200.nc
INPUT_SEVIRI_BAND03 = ../data/L1b/MSG1/2021150/MSG1_IODC___-IR_016___-202105301200.nc
INPUT_SEVIRI_BAND04 = ../data/L1b/MSG1/2021150/MSG1_IODC___-IR_039___-202105301200.nc
INPUT_SEVIRI_BAND08 = ../data/L1b/MSG1/2021150/MSG1_IODC___-IR_097___-202105301200.nc
INPUT_SEVIRI_BAND09 = ../data/L1b/MSG1/2021150/MSG1_IODC___-IR_108___-202105301200.nc
INPUT_SEVIRI_BAND10 = ../data/L1b/MSG1/2021150/MSG1_IODC___-IR_120___-202105301200.nc
INPUT_NWP = ../data/NWP/2021150/gfs.t06z.pgrb2.0p25.f006.20210530_PWAT.nc

INPUT_ALGORITHM_PARAMETERS     = ../ancillary/EFIRE_parameters_v1r2A.nc
INPUT_STATIC_METADATA          = ../ancillary/Static_Metadata.txt

OUTPUT_PREVIOUS_FIRE           = ../data/PREV_FIRES/MSG1.previousFires.nc
OUTPUT_DIRECTORY               = ../data/output
SATELLITE_ID                   = msg1
```

EFIRE Operations Manual provides example PCF files for each satellite /domain.

4.8 PSF file

EFIRE application will create a PSF file to indicate file names of output files EFIRE system created. This file will be saved in the output directory specified in PCF file.

4.9 Fire category classification

EFIRE adopted the fire category classification method in VIIRS-M fire detection algorithm. The fire pixels will be classified as 3 categories: low, medium and high confidence. Fire detection confidence was evaluated by the same function as VIIRS-VM algorithm, calculated via a combination of statistical variables, see Giglio et al. (2003) for details.

4.10 FRP calculation

The EFIRE system calculates Fire radiative power (FRP) by the method of Wooster *et al*. [2003, 2005] as described in Section 3, using coefficients specific to each satellite sensor as listed below.

Table 4-2 Coefficient of fire radiative power for each satellite

Sensor	Satellite ID	FRP constant Parameter A Unit: ×10-9 $Wm^{-2}sr^{-1}mm^{-1}K^{-4}$
VIIRS	NPP NOAA20 (J01)	2.88
	NOAA21 (J02)	2.95
ABI	G16, G17, G18	3.0
SEVIRI	MSG1, MSG2, MSG4	3.0
VII (METimage)	SGA1	3.03

4.11 Persistent anomaly flags

The EFIRE product also includes flags that indicate the presence of potential false fire detections due to non-biomass burning related radiative signal, such as reflection from solar farms, volcanos, gas flares. The flags are added based on colocation of fire detections with published or empirically determined persistent anomalies as follows:

0 – no persistent anomaly
1 - oil or gas flare (based on Liu et al., 2017)
2 – volcano (Global Volcanism Program, Smithsonian Institution, 2013)
3 – solar panel (empirically determined, CONUS only)
4 – urban (currently not used)
5 – unclassified (empirically determined)

The original persistent anomalies data was provided by in GIS format. Objects of Persistent anomalies were described as polygons. They are re-mapped into equal lat-lon grid (interval 0.0025 degree), then the latitude, longitude and category of persistent anomaly of the pixels with valid persistent anomalies were saved as 1D arrays in EFIRE parameter files.

There are a few records of volcanos in the above Persistent Anomalies in GIS database. The volcano list published on https://volcano.si.edu/volcanolist_holocene.cfm is also considered as persistent anomalies.

All persistent anomalies data sets are going to be updated routinely. After updating the data sources. EFIRE science team will provide new "EFIRE parameter file" in the same format as the latest version. While using new parameter file no code update is required.

5 EFIRE Output file

EFIRE major output product is a NETCDF file containing fire mask, quality flag, information of fire points and metadata for quality monitoring purpose.

It is optional to output information of fire points in text format.

5.1 Fire Mask

It is a byte array with the same size as 4μm BT data, indicating the result/status of fire detection for each pixel. It provided fire classification information on each pixel of input image. It is important for validation because it provides information on both fire pixel and cloud free pixels.

Figure 5-1 Legend of Fire Mask

SDS name	Meaning of value
fire_mask	#Legend of Fire Mask in VIIRS-style version 0 not-processed (non-zero QF) 1 on-board bowtie deletion 2 glint 3 water 4 clouds 5 clear land 6 unclassified fire 7 low confidence fire 8 nominal confidence fire 9 high confidence fire

Below is the image of SEVIRI MSG4 fire mask. The positions of fire pixels are marked by the "+" sign.

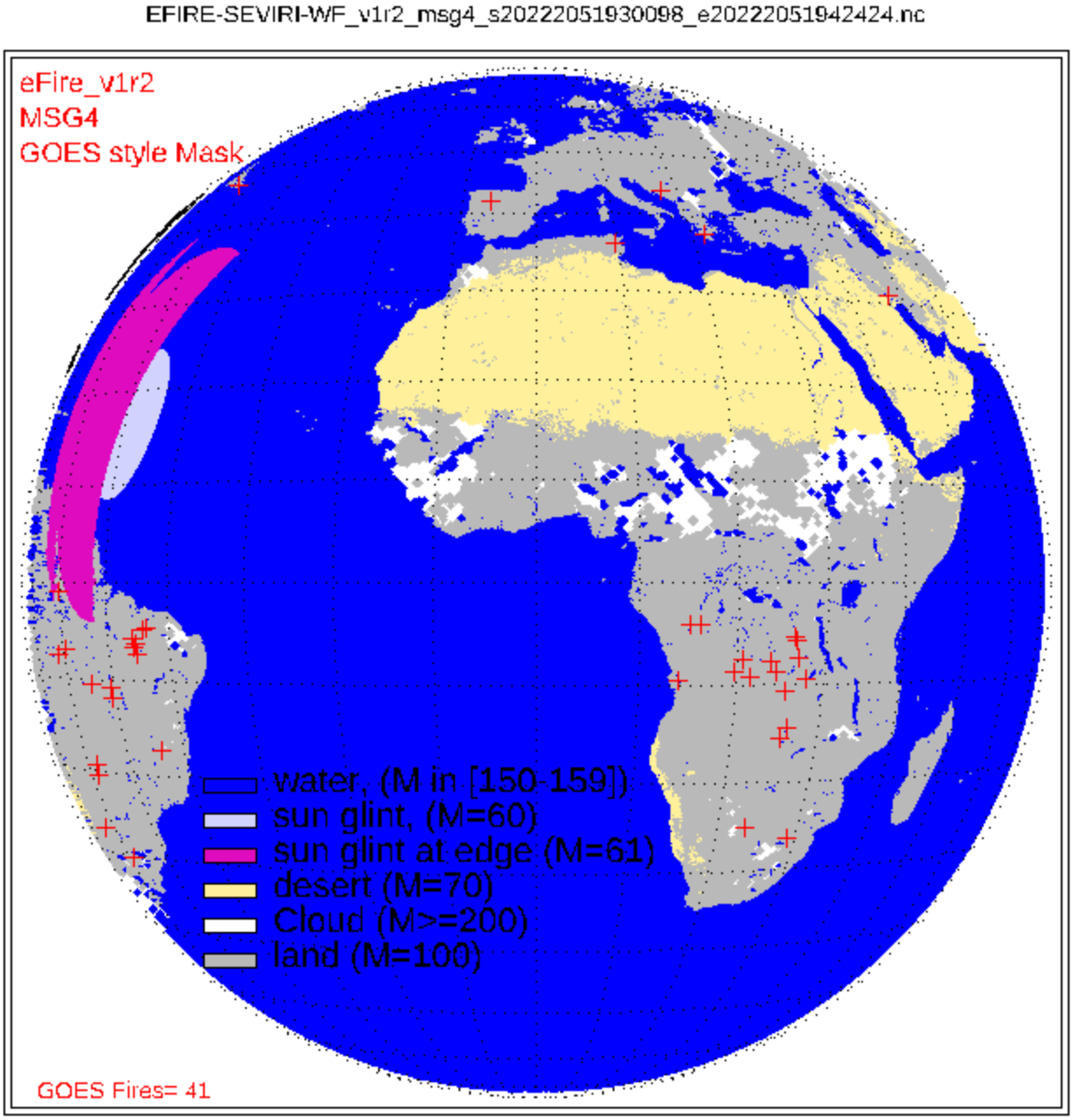

Figure 5-2 Example of Fire mask for geostationary satellite, MSG4

Below is fire mask image of a simulated METimage granule.

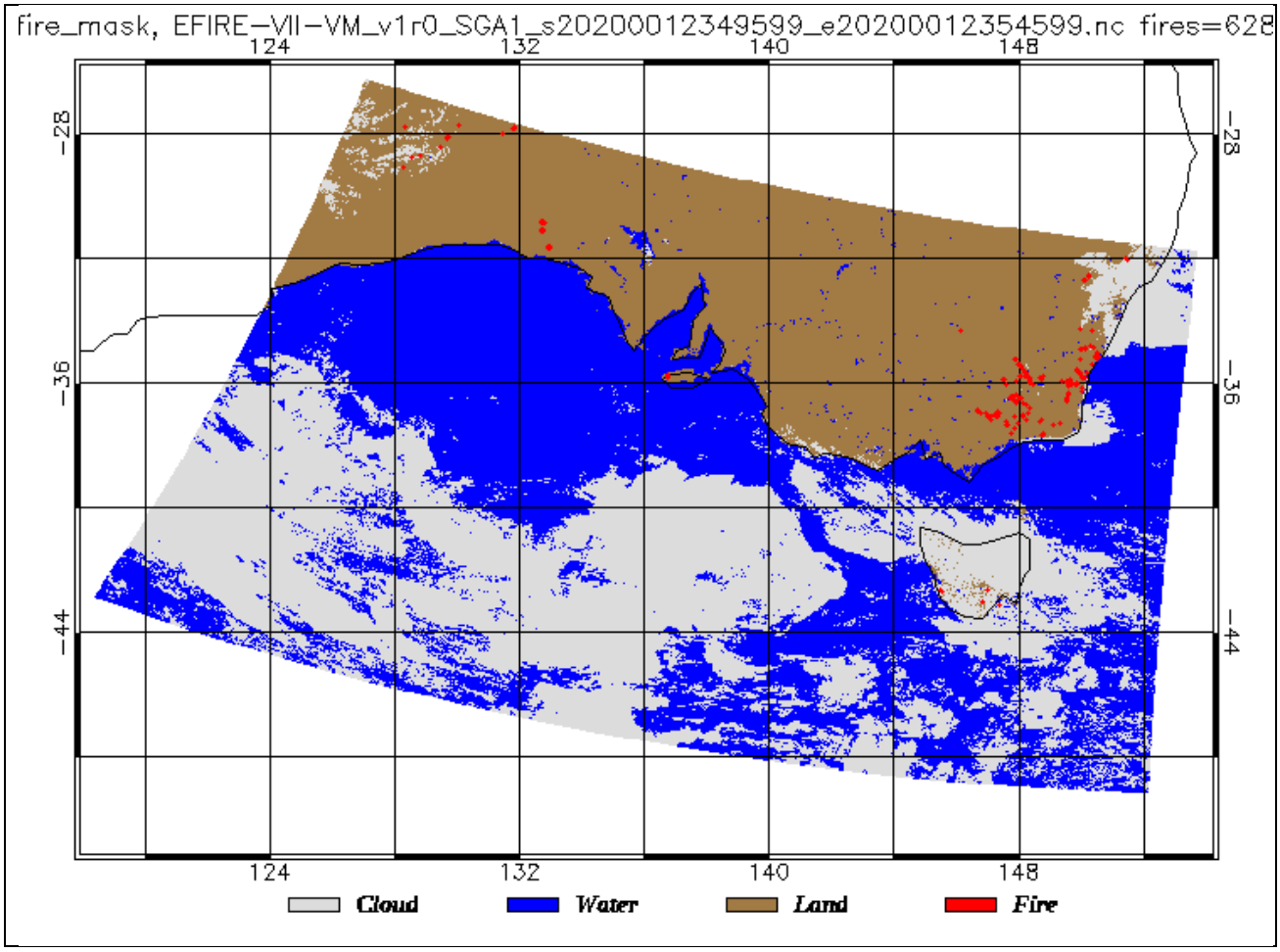

Figure 5-3 Example of Fire Mask for polar satellite, simulated METimage

5.2 Quality Flag

It is a byte array with the same size as 4μm BT data, indicating the quality of fire detection for each pixel.

Figure 5-4 Quality Flag (DQF)

SDS name	Meaning of value
DQF	#Legend of Fire QA (DQF) in GOES version 0: good_quality_fire_pixel_qf 1: good_quality_fire_free_land_pixel_qf 2: invalid_due_to_opaque_cloud_pixel_qf 3: invalid_due_to_surface_type_or_sunglint_or_LZA_threshold_exceeded_or _off_earth_or_missing_input_data_qf 4: invalid_due_to_bad_input_data_qf 5: invalid_due_to_algorithm_failure_qf

Pxiel level fire retrirval qaulity of EFIRE product will be saved in “DQF” array.

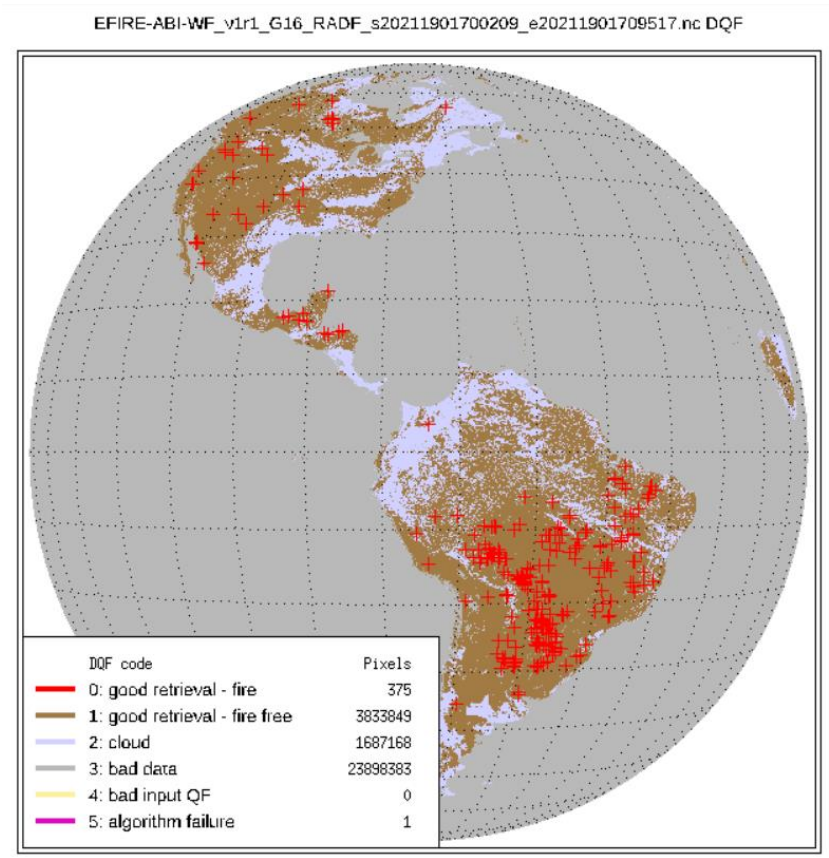

Figure 5-5 Example image of DQF

In VIIRS option, the quality flags are defined as a byte array (QA) with the same size as 4um BT data. The content of QA for M-band and I-band is described in corresponding ATBDs.

5.3 Information of fire points

These are a group of 1D arrays stored the information of fire points. One variable per array. The SDS name starts with "FP_". It may include latitude, longitude, Fire radiative power, Fire sun pixel area, BT value of each bands, Persistent Anomalies type and time tag and other related variables.
The variable names were provided by generic names (avoiding the sensor band specific names).

Example:

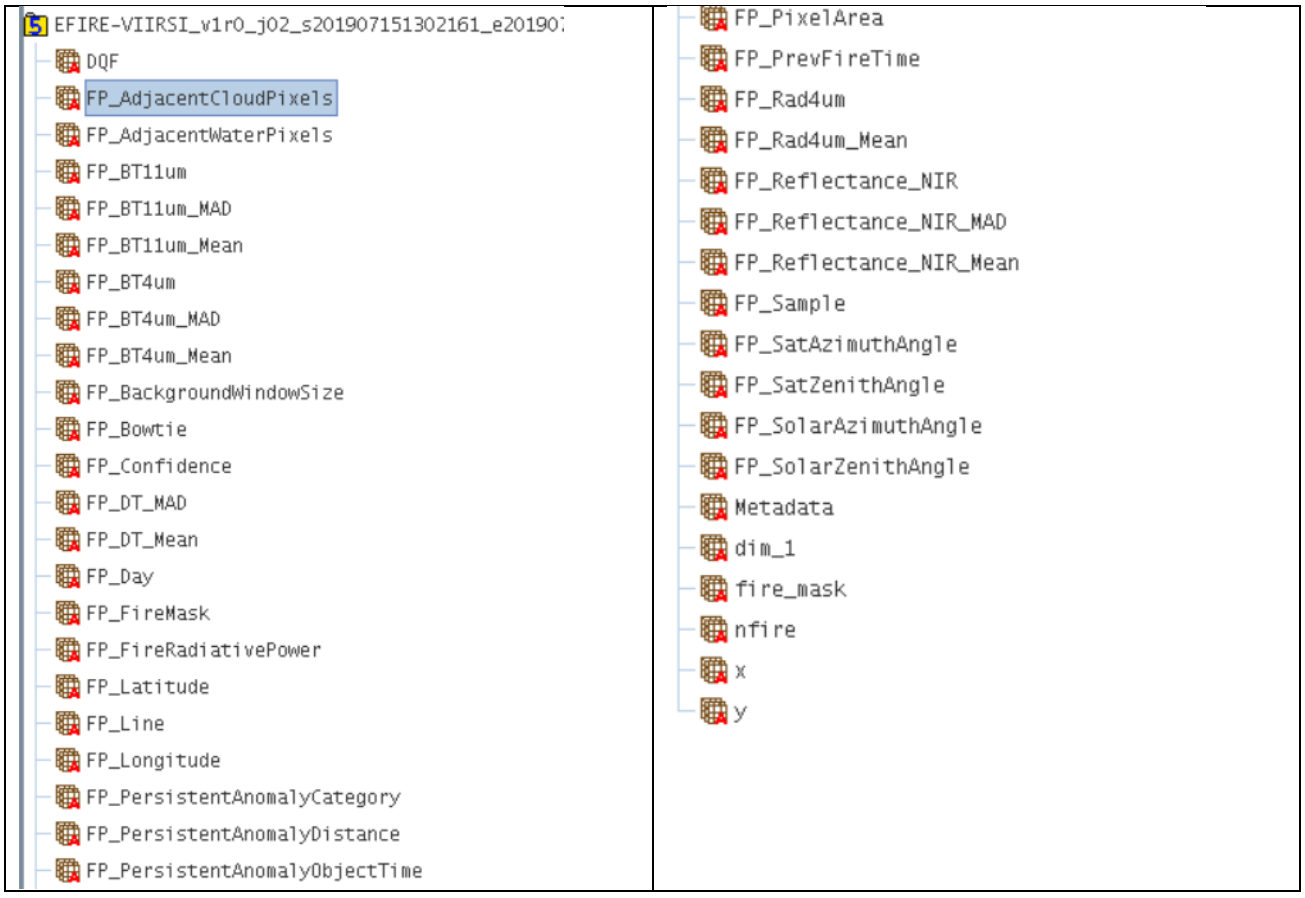

Figure 5-6 Variables of fire pixels

5.4 Metadata

Granule level metadata are saved as attributes of SDS “Metadata”. They contain the number of pixels for various categories. Here is an example of granule level metadata as it appears in HDFview.

Table 5-1 Metadata (Example)

Name	Value
CloudAdjacentFire_pixels	2
Cloud_pixels	1152888
CoastRejectLand_pixels	2
CoastRejectWater_pixels	0
DIMENSION_LIST	3179
Daytime_pixels	8342603
Fire_pixels	50
Fires_Rejected_Forest	0
GlintReject_pixels	2
Glint_pixels	0
HotReject_pixels	0
LandCloud_pixels	1152888
LandFire_pixels	50
Land_pixels	3732163
MissingGeo_pixels	3498123
MissingRad_pixels	3579360
Missing_pixels	150298
Night_pixels	5286043
NoFire_pixels	6836413
UnknownLandFire_pixels	0
UnknownWaterFire_pixels	16092
WaterAdjacentFire_pixels	0
WaterCloud_pixels	0
WaterFire_pixels	0
Water_pixels	9896483
fire_pixels_mask_7	262
fire_pixels_mask_8	1620
fire_pixels_mask_9	706
mask_0_unprocessed_pe...	1.0907803
mask_4_cloud_pixel_perc...	8.367027
mask_7_fire_percent	6.531705E-5
mask_8_fire_percent	2.757831E-4
mask_9_fire_percent	2.177235E-5
max_detections_col	2
max_detections_row	3
mean_frp	7.9360374E11
total_frp	3.9680188E13

5.5 Fire product in text format

Fires detected can also be saved in text format.
It records the following information of each fire point: the observation time, latitude, longitude, fire mask, confidence BT of 4μm band, fire radiative power (FRP), position (line and sample) in input array, is a bowtie pixel or not (it is meaningful for polar satellite only), and category for persistent anomalies (0: not a persistent anomaly).

Below is an example of ASCII file format (for testing case of J02).

Figure 5-7 Example of fire product in ASCII format

```
year,month,day,hh, mm,lon,lat,mask,confidence,bright_t4,frp,line,sample,bowtie,persist_anomaly;  nfire = 386
 2019, 07, 15, 13, 03, -143.097076,   67.282494,   8, -99,  353.033173,   17.995117,  1127,  4121,   0,   0
 2019, 07, 15, 13, 03, -143.111908,   67.281738,   8, -99,  327.145050,    6.747824,  1128,  4120,   0,   0
 2019, 07, 15, 13, 03, -143.102402,   67.279388,   8, -99,  339.051788,    6.747824,  1128,  4121,   0,   0
 2019, 07, 15, 13, 03, -143.092819,   67.277031,   8, -99,  330.736237,    5.287928,  1128,  4122,   0,   0
 2019, 07, 15, 13, 03, -143.164963,   67.290352,   8, -99,  325.089813,    3.949202,  1129,  4115,   0,   0
 2019, 07, 15, 13, 03, -143.148453,   66.906815,   8, -99,  328.547546,    5.690307,  1225,  4164,   0,   0
 2019, 07, 15, 13, 03, -143.208298,   66.903900,   8, -99,  334.193970,    4.231627,  1229,  4160,   0,   0
 2019, 07, 15, 13, 03, -143.150116,   66.880417,   8, -99,  326.887848,    3.479891,  1231,  4167,   0,   0
 2019, 07, 15, 13, 03, -143.248703,   66.878311,   8, -99,  337.147003,    8.176878,  1237,  4160,   0,   0
 2019, 07, 15, 13, 03, -143.239380,   66.867043,   8, -99,  340.582916,    8.133868,  1239,  4162,   0,   0
 2019, 07, 15, 13, 03, -143.273682,   66.871178,   8, -99,  337.814301,   11.636395,  1240,  4159,   0,   0
```

6 TEST DATA SETS AND OUTPUTS

EFIRE Algorithm verification and validation is limited due to the lack of comprehensive "truth" data sets that provide simultaneous observations of actively burning fires at the time of the satellite information. Cross comparison of fire products derived from various satellites is a major validation method. Usually, the product with higher resolution is more helpful to validate fire product with coarser resolution.

EFIRE products were tested by comparing EFIRE product to previous versions of fire product (current official product of ABI (WF_ABBA), VIIRS-M, VIIRS-I, MODIS etc.).

6.1 Verification of EFIRE products generated by the VIIRS-I and VIIRS-M Algorithms

EFIRE implemented VIIRS-I and VIIRS-M by directly merging the original codes. Several modifications are done for integration of the codes into EFIRE, including the following:

- Big buffer (the size of input granule) is used in VIIRS-M instead of processing granule scan by scan with small buffers (heritage of the original M-band algorithm design for limited memory platforms; the baseline I-band is already using granule size buffer).
- Shared input/output module for both VIIRS-M and VIIRS-I is used in EFIRE
- Output is generated using common names and formats
- Integrated VIIRS-I and VIIRS-M utilize EFIRE consistent memory management including checking size before memory allocation

Also, EFIFE defines land-water mask by using code/procedure different from the baseline M-band and I-band algorithms - which may result in slightly different output fire product. For verification purposes, however, EFIRE was run with the land-water mask used in the baseline/operational processing. The test runs show that with identical land-water mask, EFIRE produces exactly the same ASCII output (i.e. the same fire pixels were detected and characterized). The testing details are listed below.

6.1.1 Testing case for VIIRS-M fire detection algorithm

Verification included one test granule. In an output of EFIRE run, 79 fire pixels were detected, the exact same result as the original M-band run.

Below is the PCF file and output file name.

```
INPUT_SVM13=../data/input/SVM13_j01_d20191010_t2250451_e2252096_b09812_c20191010233145644727_noac_ops.h5
INPUT_SVM15=../data/input/SVM15_j01_d20191010_t2250451_e2252096_b09812_c20191010233145738955_noac_ops.h5
INPUT_SVM16=../data/input/SVM16_j01_d20191010_t2250451_e2252096_b09812_c20191010233145769345_noac_ops.h5
INPUT_SVM05=../data/input/SVM05_j01_d20191010_t2250451_e2252096_b09812_c20191010233145973563_noac_ops.h5
INPUT_SVM07=../data/input/SVM07_j01_d20191010_t2250451_e2252096_b09812_c20191010233146096892_noac_ops.h5
INPUT_SVM11=../data/input/SVM11_j01_d20191010_t2250451_e2252096_b09812_c20191010233145559406_noac_ops.h5
INPUT_GMTCO=../data/input/GMTCO_j01_d20191010_t2250451_e2252096_b09812_c20191010233050343464_noac_ops.h5
INPUT_LWMSK=../data/input/AF-LAND_MASK_NASA_1KM_s201910102250451_e201910102252096_c201910152150580.nc
INPUT_ALGORITHM_PARAMETERS=../ancillary/eFire_parameters_v1r2A.nc
INPUT_STATIC_METADATA=../ancillary/Static_Metadata.txt
OUTPUT_PREVIOUS_FIRE=../data/PREV_FIRES/j01.PersistentWaterFireRef.txt
OUTPUT_FIRE_NETCDF=PROD
ALGORITHM=VIIRS-VM
SATELLITE_ID=j01
[END]

saveFileContentAsAttribute() attr_name=PCF_FILE_CONTENT file=../run_SAT/v1r2/vfire_VM.pcf
saved, file= ../data/output/VIIRS-VM_j01/2019283/EFIRE-VIIRS-VM_v1r2_j01_s20192832250451_e20192832252096.nc
```

6.1.2 Testing case for VIIRS-I fire detection algorithm

Two granules (daytime and nighttime) are tested.

For the daytime case, 474 fires were detected, the same result as original I-band code.

```
INPUT_SVI01=../data/input/SVI01_j01_d20181108_t2039164_e2040410_b05044_c20181108210815004280_nobc_ops.h5
INPUT_SVI02=../data/input/SVI02_j01_d20181108_t2039164_e2040410_b05044_c20181108210815010737_nobc_ops.h5
INPUT_SVI03=../data/input/SVI03_j01_d20181108_t2039164_e2040410_b05044_c20181108210815017710_nobc_ops.h5
INPUT_SVI04=../data/input/SVI04_j01_d20181108_t2039164_e2040410_b05044_c20181108210815024511_nobc_ops.h5
INPUT_SVI05=../data/input/SVI05_j01_d20181108_t2039164_e2040410_b05044_c20181108210815031609_nobc_ops.h5
INPUT_SVM13=../data/input/SVM13_j01_d20181108_t2039164_e2040410_b05044_c20181108210853337168_nobc_ops.h5
INPUT_IVCDB=../data/input/IVCDB_j01_d20181108_t2039164_e2040410_b05044_c20181108210815098248_nobc_ops.h5
INPUT_GITCO=../data/input/GITCO_j01_d20181108_t2039164_e2040410_b05044_c20181108210715103775_nobc_ops.h5
INPUT_LWMSK=../data/input/AF-LAND_MASK_NASA_1KM_s201811082039164_e201811082040410_c201811301957410.h5
INPUT_ALGORITHM_PARAMETERS=../ancillary/eFire_parameters_v1r2A.nc
INPUT_STATIC_METADATA=../ancillary/Static_Metadata.txt
OUTPUT_PREVIOUS_FIRE=../data/PREV_FIRES/j01.PersistentWaterFireRef.txt
OUTPUT_FIRE_NETCDF=PROD
ALGORITHM=VIIRS-I
SATELLITE_ID=j01
[END]

saveFileContentAsAttribute() attr_name=PCF_FILE_CONTENT file=../run_SAT/v1r2/vfire375_day.pcf
saved, file= ../data/output/VIIRS-I_j01/2018312/EFIRE-VIIRS-I_v1r2_j01_s20183122039164_e20183122040410.nc
```

For the nighttime testing case, 60 fires were detected, the same result as original I-band code.

It should be noted that the I-band algorithm creates a reference file with some information about previous fires at water locations (oil/gas platforms). The file is updated with every run and intended to be used primarily in near real-time processing. When comparison tests are performed, and especially for limited number of granules – it is important to have the same reference file at start, either by setting it to zero or using the same content, e.g., from existing real-time processing. If the same granule is processed several times in tests, each subsequent run makes unnecessary/unrealistic updates to the reference file (treating fires detected in previous run for the same granule as “previous fires”). This may result in discrepancy in outputs and make difficult to compare baseline I-band and VIIRS-I EFIRE. In this particular granule, one fake fire pixel (61 total, with 60 in I-band) over water was detected by EFIRE due to the same granule reprocessing in tests.

```
INPUT_SVI01=../data/input/SVI01_j01_d20190829_t0036008_e0037253_b09203_c20190829011745755661_nobc_ops.h5
INPUT_SVI02=../data/input/SVI02_j01_d20190829_t0036008_e0037253_b09203_c20190829011745767871_nobc_ops.h5
INPUT_SVI03=../data/input/SVI03_j01_d20190829_t0036008_e0037253_b09203_c20190829011745775890_nobc_ops.h5
INPUT_SVI04=../data/input/SVI04_j01_d20190829_t0036008_e0037253_b09203_c20190829011745785648_nobc_ops.h5
INPUT_SVI05=../data/input/SVI05_j01_d20190829_t0036008_e0037253_b09203_c20190829011745795539_nobc_ops.h5
INPUT_SVM13=../data/input/SVM13_j01_d20190829_t0036008_e0037253_b09203_c20190829011809937139_nobc_ops.h5
INPUT_IVCDB=../data/input/IVCDB_j01_d20190829_t0036008_e0037253_b09203_c20190829011745751165_nobc_ops.h5
INPUT_GITCO=../data/input/GITCO_j01_d20190829_t0036008_e0037253_b09203_c20190829011650583841_nobc_ops.h5
INPUT_LWMSK=../data/input/AF-LAND_MASK_NASA_1KM_s201908290036008_e201908290037253_c201908290132320.h5
INPUT_ALGORITHM_PARAMETERS=../ancillary/eFire_parameters_v1r2A.nc
INPUT_STATIC_METADATA=../ancillary/Static_Metadata.txt
OUTPUT_PREVIOUS_FIRE=../data/PREV_FIRES/j01.PersistentWaterFireRef.txt
OUTPUT_FIRE_NETCDF=PROD
ALGORITHM=VIIRS-I
SATELLITE_ID=j01
[END]

saveFileContentAsAttribute() attr_name=PCF_FILE_CONTENT file=../run_SAT/v1r2/vfire375_night.pcf
saved, file= ../data/output/VIIRS-I_j01/2019241/EFIRE-VIIRS-I_v1r2_j01_s20192410036008_e20192410037253.nc
```

6.2 Verification of the ABI or SEVIRI EFIRE product

6.2.1 Validation procedure

ABI/SEVIRI EFIRE product was generated and compared to VIIRS fire products.
There are 4 datasets of operational VIIRS fire products:

- VIIRSM-NPP: Fire product from VIIRS NPP by using “VIIRS-M” fire detection algorithm.
- VIIRSM-J01: Fire product from VIIRS J01 by using “VIIRS-M” fire detection algorithm.
- VIIRSI-NPP: Fire product from VIIRS NPP by using “VIIRS-I” fire detection algorithm.
- VIIRSI-J01: Fire product from VIIRS J01 by using “VIIRS-I” fire detection algorithm.

The code for validating ABI/SEVIRI data by VIIRS fire product follows the procedure below:

- The time matched ABI/SEVIRI image file and VIIRS granule was searched by threshold of time separation (5.0 minutes for ABI and 7.5 minutes for SEVIRI),
- Pixels of this VIIRS granule was mapped onto ABI/SEVIRI full disk domain; multiple VIIRS pixel may go into one ABI/SEVIRI pixel;
- For a given ABI/SEVIRI pixel, we will count the number of VIIRS fire pixels and cloud free land pixels falling into this pixel, and save the daily matched fire masks and records the daily statistics on confirm rate, false alarm rate and detection rate for day time and night time respectively.

Confirm rate indicates the percent of ABI/SEVIRI fire pixels that can be verified by VIIRS fire (at least 1 VIIRS fire pixel falls into a given ABI/SEVIRI fire pixel).

False alarm rate is percent of ABI/SEVIRI fire pixels that cannot be verified by VIIRS fire (at least 1 VIIRS cloud free pixel fall into a given ABI/SEVIRI fire pixel, but none of them was identified as VIIRS fire).

Detection rate evaluates the capability of ABI/SEVIRI fire product to catch big fire. Fire size was defined as the number of VIIRS pixels in an ABI/SEVIRI pixel.

6.2.2 Flowchart of Validating the EFIRE ABI/SEVIRI fire product by using the VIIRS fire product

Below is the detailed processing procedure for validating fire product from geostationary satellites (ABI/SEVIRI) by VIIRS fire product:

- We need fire mask (2D) arrays in ABI/SEVRI and VIIRS fire product. The fire mask can provide information

1) where the fire pixels are located
2) where the non-fire cloud free land pixels are located.

- Inputs from ABI/SEVIRI fire product:
  - fire mask from EFIRE or Fire generated by WF_ABBA (OR fire files on SCDR).
  - For EFIRE, both GOES style fire mask (G-Mask, 12 classes for fire, [10~15,30~35]) and VIIRS style fire mask (V-Mask, 3 classes for fire: 7,8,9) are available. For Fire generated by WF_ABBA, only GOES style fire mask (G-Mask, 12 classes for fire, [10~15,30~35]) are available
  - The validation procedure will process when both fire product files from EFIRE and WF_ABBA for a given image are available.
  - There are about 96 images/day for SEVIRI; 144 images /day for ABI
- Geolocation file for ABI/SEVIRI full disk domain;
  - static files (not change unless the satellite is moved to new location.
  - can be generated by EFIRE system,
  - need be verified before using them (make sure the satellite position is consistent to Fire product).
- VIIRS fire file:
  - contains VIIRS style fire mask (V-Mask, 3 classes for fire: 7,8,9)
  - about 1014 granules /day, ¼ of them may match with ABI or SEVIRI domain
- VIIRS geolocation:
  - GITCO or GMTCO file
  - large file
  - about 1014 granules /day, about ¼ of them need to be processed for a given ABI or SEVIRI domain
- Time match:
  - Image middle time of ABI/SEVIRI or VIIRS image is calculated from starting and ending time.
  - If time separation of ABI/SEVIRI and VIIRS < threshold, they are time-matched:

  For ABI and VIIRS, time separation should < 5 minutes
  For SEVIRI and VIIRS, time separation should < 7.5 minutes

- For time matched images:
  - Process daytime and night separately
  - Map VIIRS pixels to ABI/SEVIRI domain
  - Count number of VIIRS fire pixels in each ABI /SEVIRI pixel
  - Record the Fire mask and time of G-pixel
  - Statistics for each Fire class
  - Generate one daily validation result file (HDF) per day
- Generate summary report from multiple days' daily validation result file (HDF).
  - Generate validation scores based on V-mask
  - Generate validation scores based on G-mask so that we can compare the validation result between fires from EFIRE and WF_ABBA.

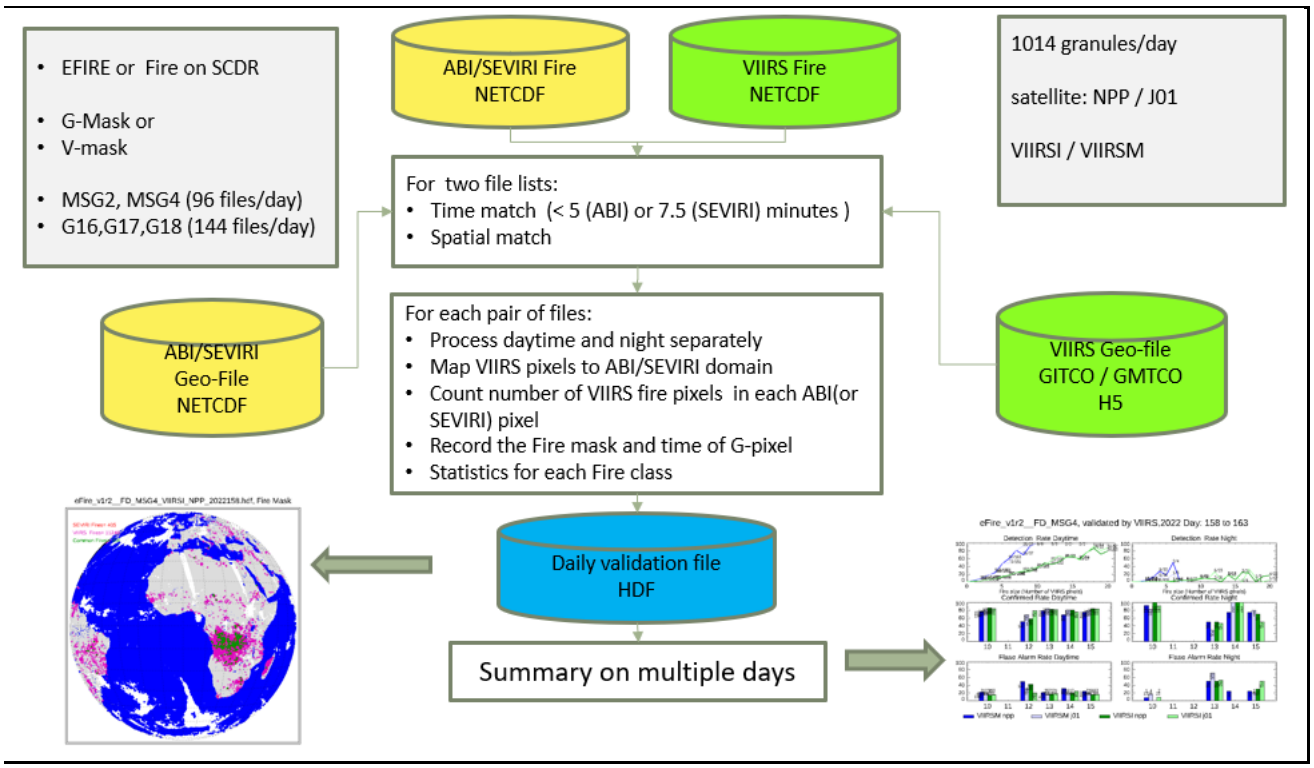

Figure 6-1 Flowchart of validating Geostationary (ABI/SEVIRI) fire product by VIIRS fire product.

6.2.3 Daily composite fire mask

It is optional to create daily composite fire mask overlaid with ABI/SEVIRI fire pixels (red) and VIIRS fire pixels (pink) and common fire pixels (green). The purpose is to verify the procedure work well and shows the distribution of fires detected.

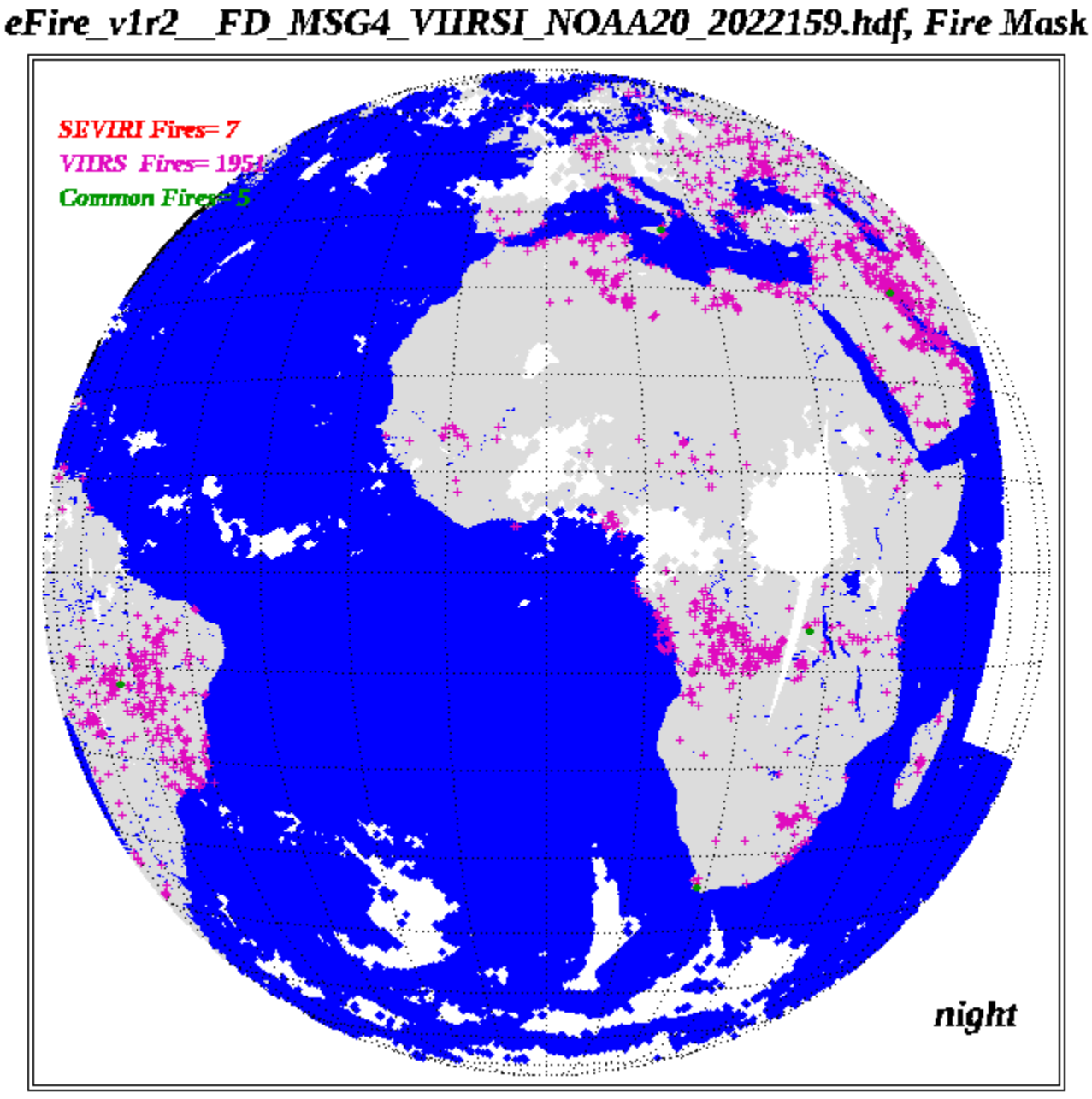

Figure 6-2 Daily composite fire mask overlaid with ABI/SEVIRI fire pixels (red) and VIIRS fire pixels (pink) and common fire pixels (green).

6.3 Validation of SEVIRI EFIRE product by VIIRS fire product

SEVIRI EFIRE product was validated by VIIRS fire products by using 50 days' data from DOY 158 to 207, 2022. MSG2 or MSG4 fire data set was compared to 4 VIIRS fire products respectively.

- The validation scores for MSG2 and MSG4 is very similar.
- The confirm rate is high, about 80% for low, medium and high confidence fire (Fire class=7,8 and 9) for daytime and night respectively. There is no obvious difference in confirm rate for the 3 fire classes.
- Detection rate is much lower at night than daytime even for big fire, which means either SEVIRI fire detector does not catch VIIRS-I fires or VIIRS-I algorithm overestimates them. The issue requires further investigation We also generated validation result by using short data period (6, 21, and 35 days). The validation result using 21 and 25 days are quite similar to that using 50 days' data. This suggests that we can use the validation result using data of 21 days or longer period.

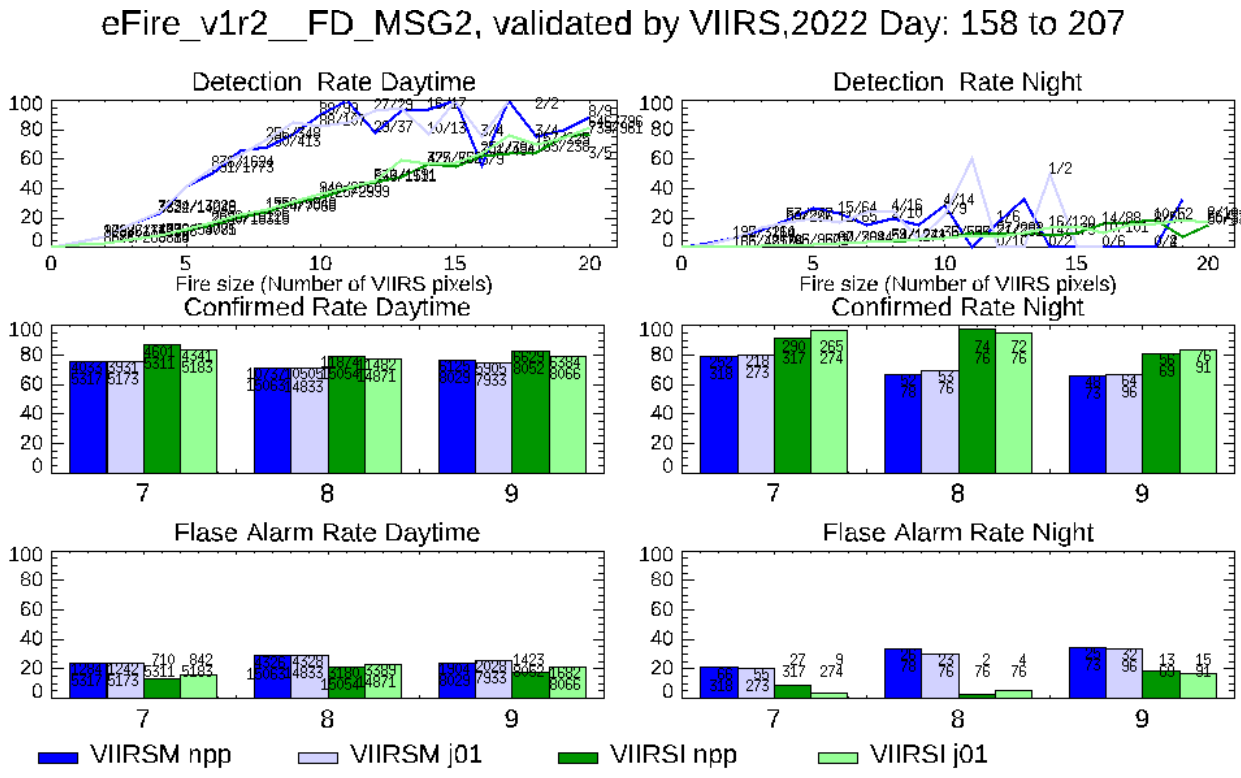

Figure 6-3 Result of validating SEVIRI MSG2 fire product by VIIRS fire product using data DOY 158-207, 2022

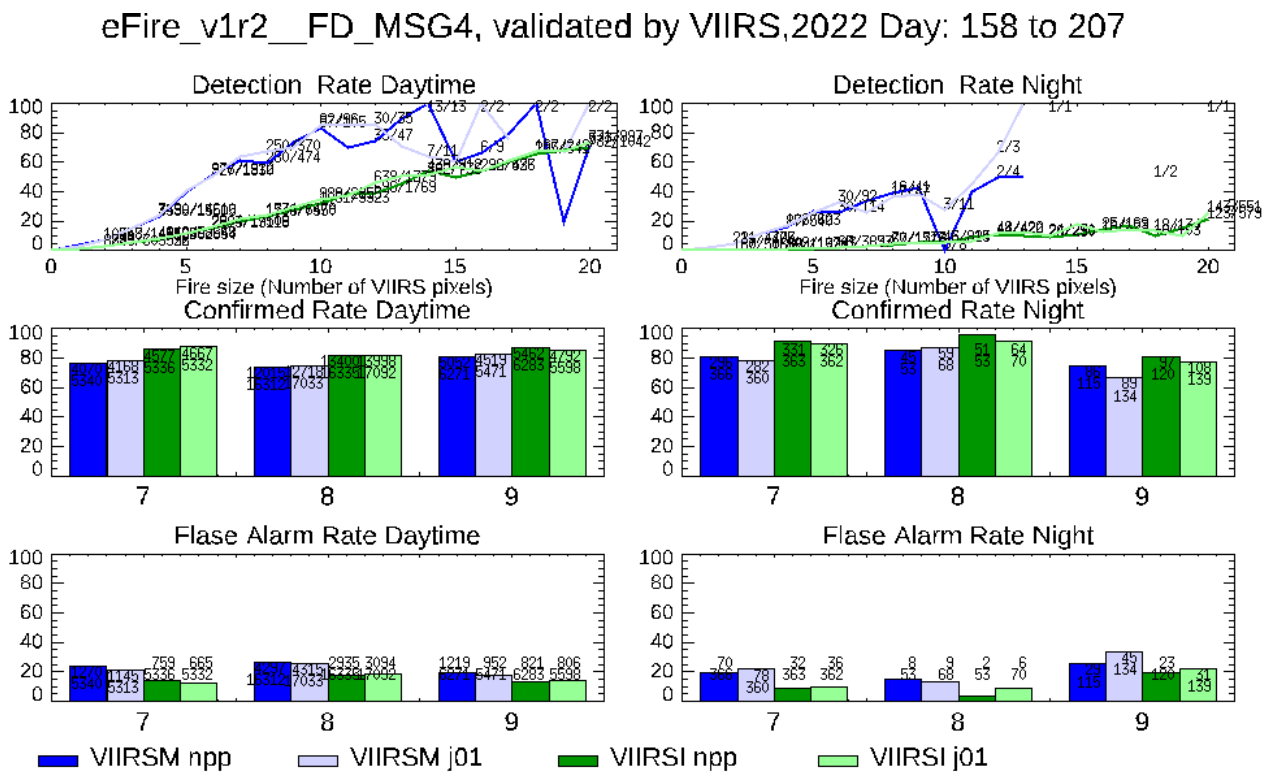

Figure 6-4 Result of validating SEVIRI MSG4 fire product by VIIRS fire product using data DOY 158-207,2022

6.4 Validation of EFIRE ABI fire by VIIRS product

ABI EFIRE product was also validated by VIIRS fire products by using 50 days' data from DOY 158 to 207, 2022. EFIRE data sets of G16, G17 and G18 were compared to 4 VIIRS fire products respectively.

The following were noticed:

- In general, the confirm rate of G16 fire is much higher than G17 and G18. For G17 and G18, most of pixels for validation are located off nadir, have large satellite zenith angle. Off nadir observations have longer optical length through the atmosphere, easier to be affected by cloud, water vapor and aerosol. It is reasonable for G17 and G18 to have less confirm rate.
- The relationship between the confirm rate and detection confidence (fire class) of G16 fire is obvious: G16 fires with high detection confidence (class 9) have higher confirm rate than those with low detection confidence (class 7). This is true for all there ABI satellites (G16, G17, and G18).
  ABI fires detected by nighttime image have larger confirm rates than ABI daytime fires.

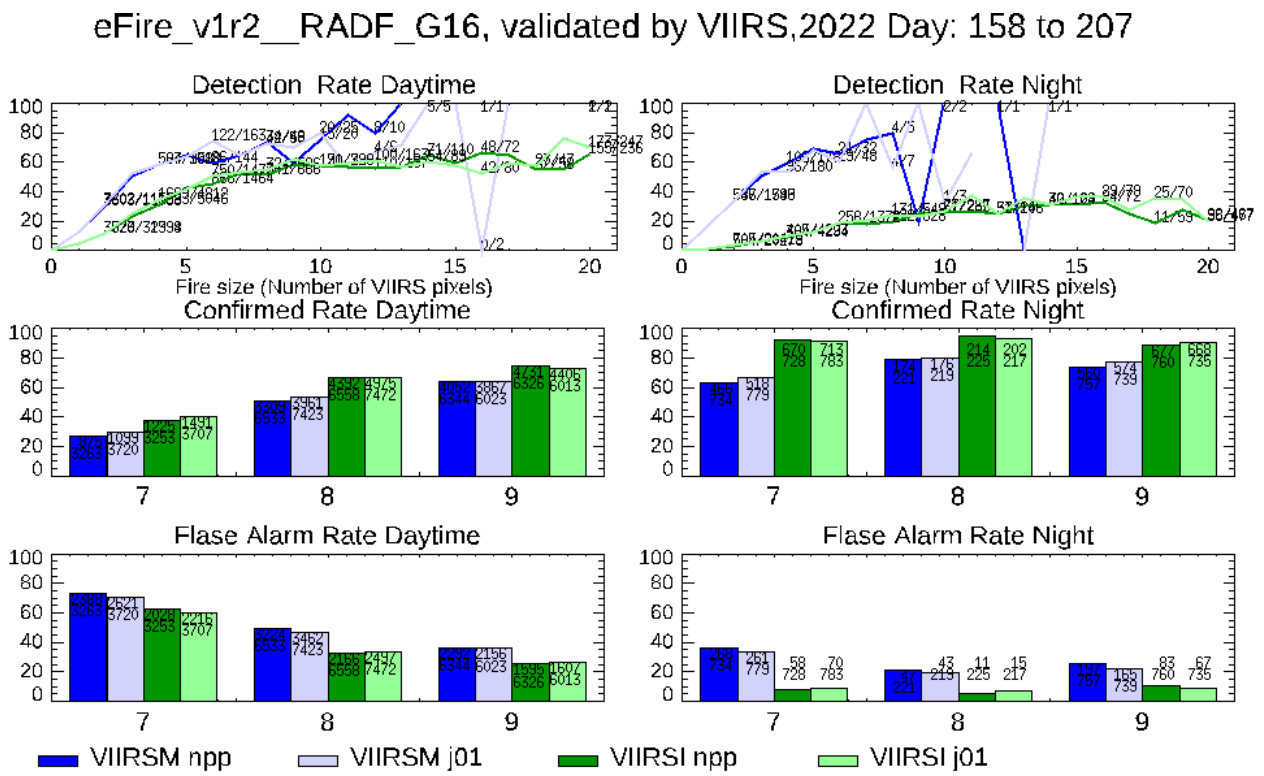

Figure 6-5 Result of validating G16 ABI fire product by VIIRS fire product using data DOY 158-207,2022

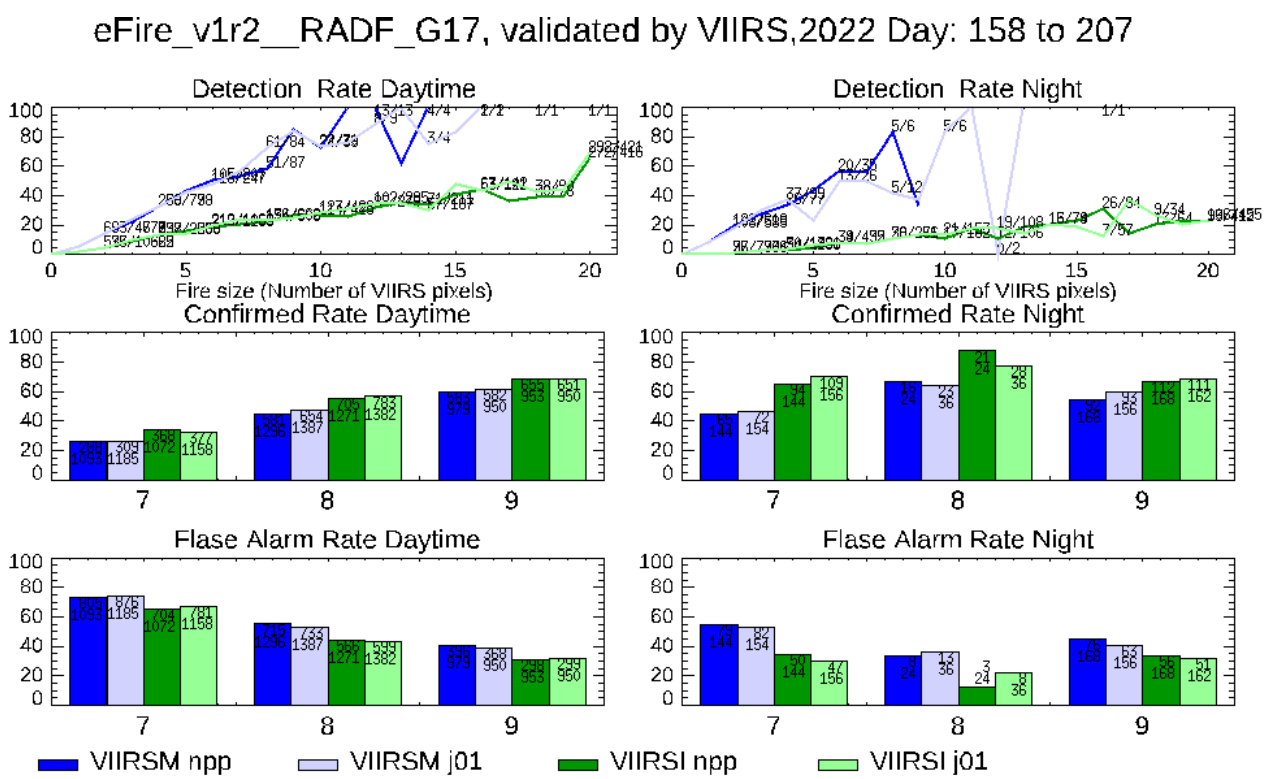

Figure 6-6 Result of validating G17 ABI fire product by VIIRS fire product using data DOY 158-207,2022

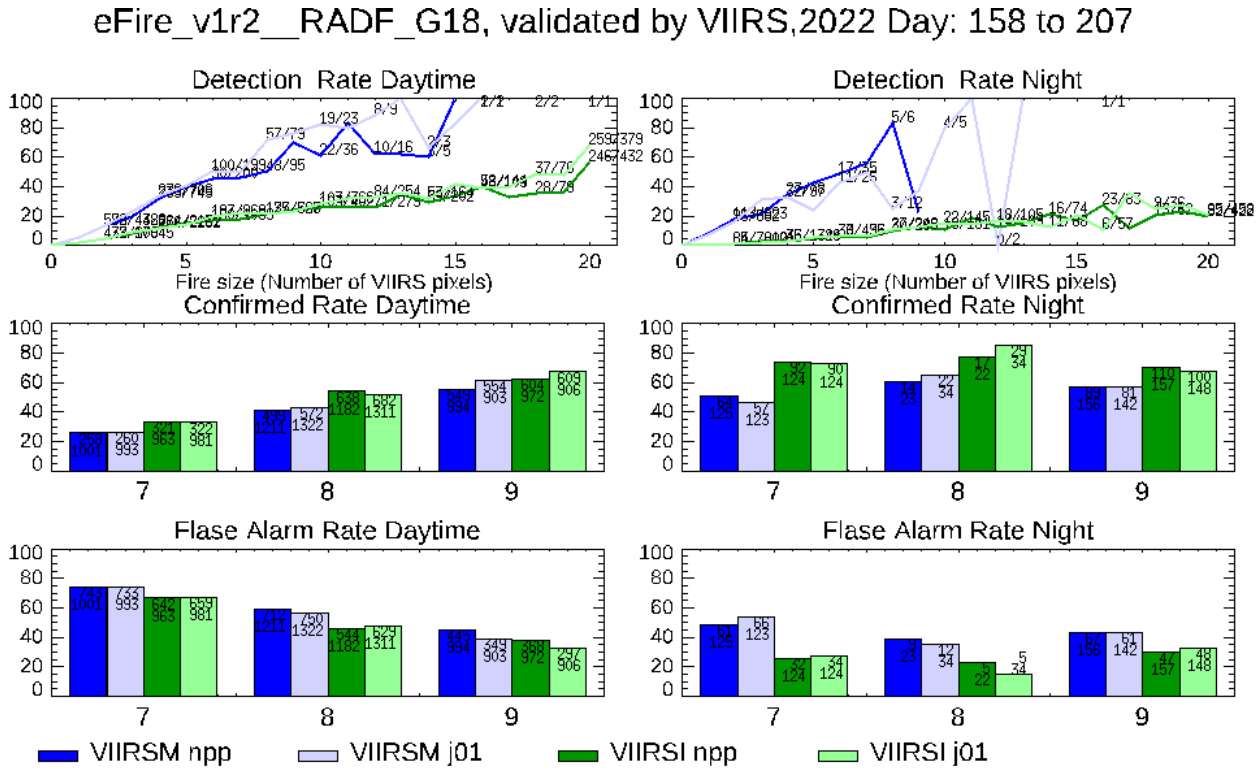

Figure 6-7 Result of validating G18 ABI fire product by VIIRS fire product using data DOY 158-207,2022

6.5 Comparing EFIRE and WF_ABBA when validating ABI fire product by VIIRS fire

Fire product generated by WF_ABBA algorithm ("OR" file on SCDR) contains only GOES style fire mask (12 classes). For comparison purposes, EFIRE was set to also save GOES style fire mask. The validation cores/plots were created for the 6 fire classes after merging time-filter fire classes (class 30 to 35) to normal fire classes (class 10 to 15). Statistics was carried out by using the ABI images which are available in both EFIRE and WF_ABBA fire dataset.

The validation result of daytime is consistent for EFIRE and WF_ABBA. Because the major difference between the EFIRE and WF_ABBA is that EFIRE removed huge number of false alarms due to sun glint at edge of full disk. Such false alarms occurred at local morning time. Thus, daytime validation scores will not be affected.

The nighttime validation plots on ABI fire products from EFIRE and WF_ABBA illustrate obvious differences, especially on the fire class 15. WF_ABBA produced huge number of fires with low detection confidence (fire class 15) but the confirm rate of them is very low (near 0). This is because false alarms due to sun glint were included in the validation samples at night.

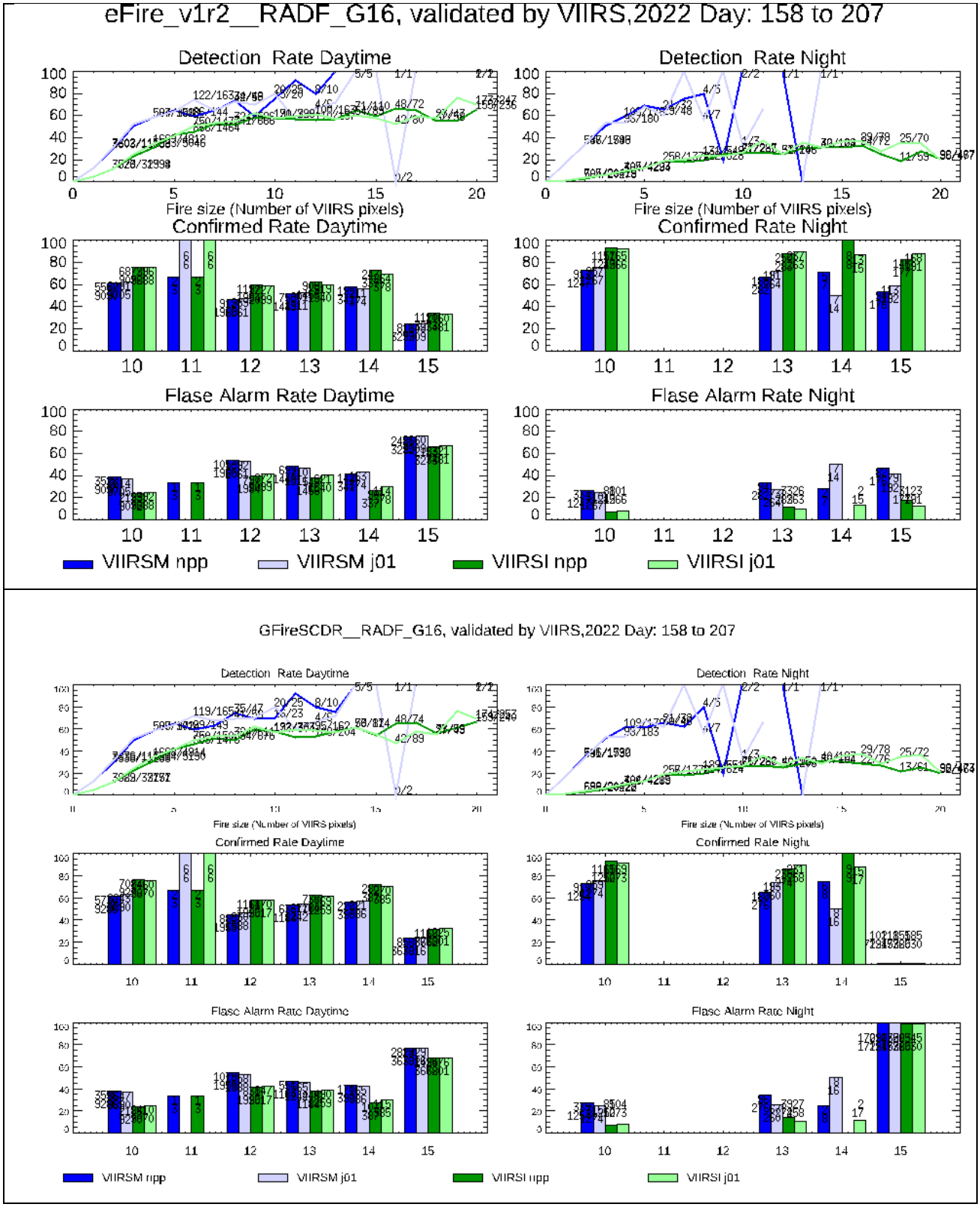

Figure 6-8 Comparing validation results of G16 ABI fire product derived by EFIRE (top) and WF_ABBA (OR files from SCDR, bottom) by VIIRS fire product using data DOY 158-207,2022

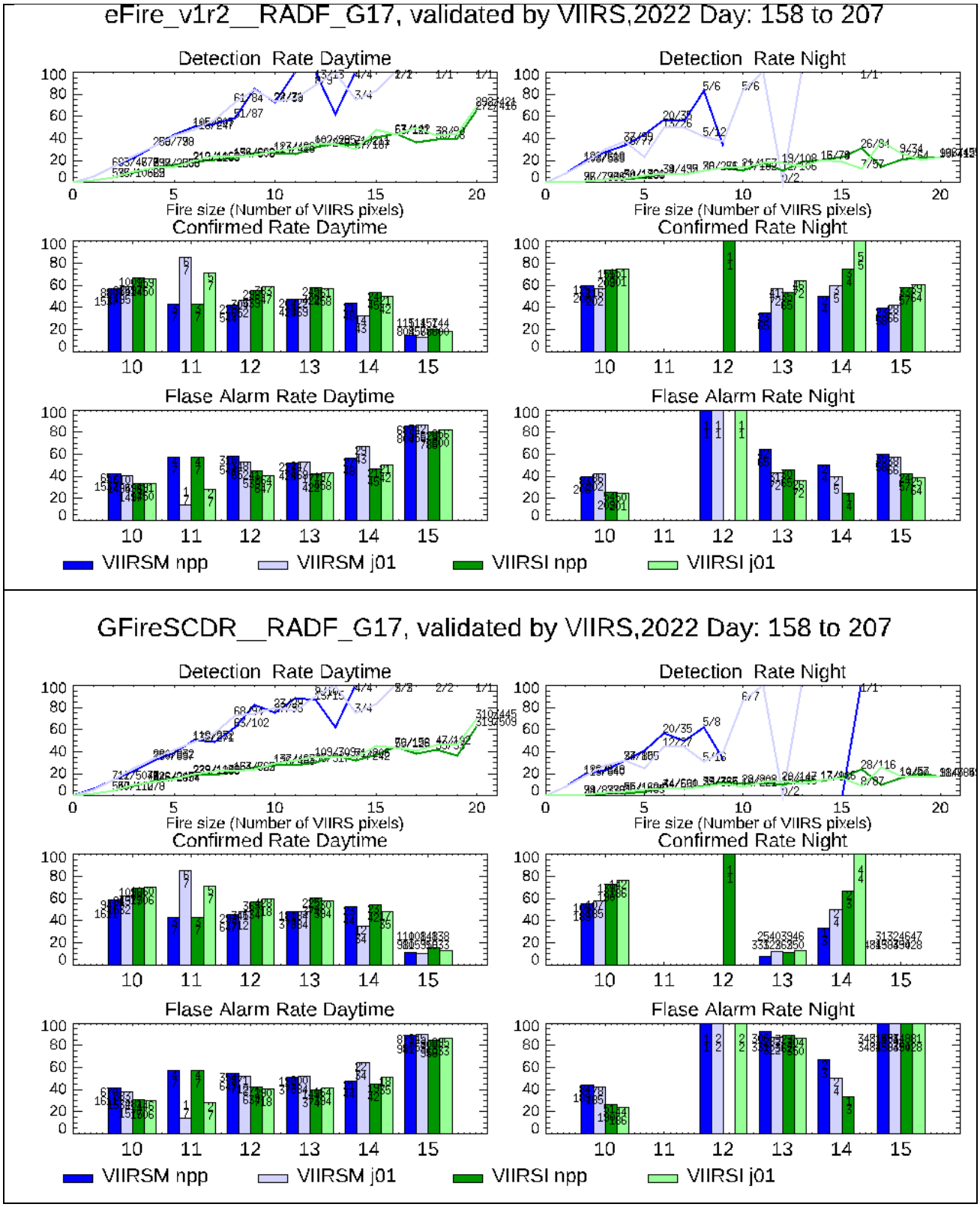

Figure 6-9 Comparing validation results of ABI G17 fire product derived by EFIRE (top) and WF_ABBA (OR files from SCDR, bottom) by VIIRS fire product using data DOY 158-207, 2022

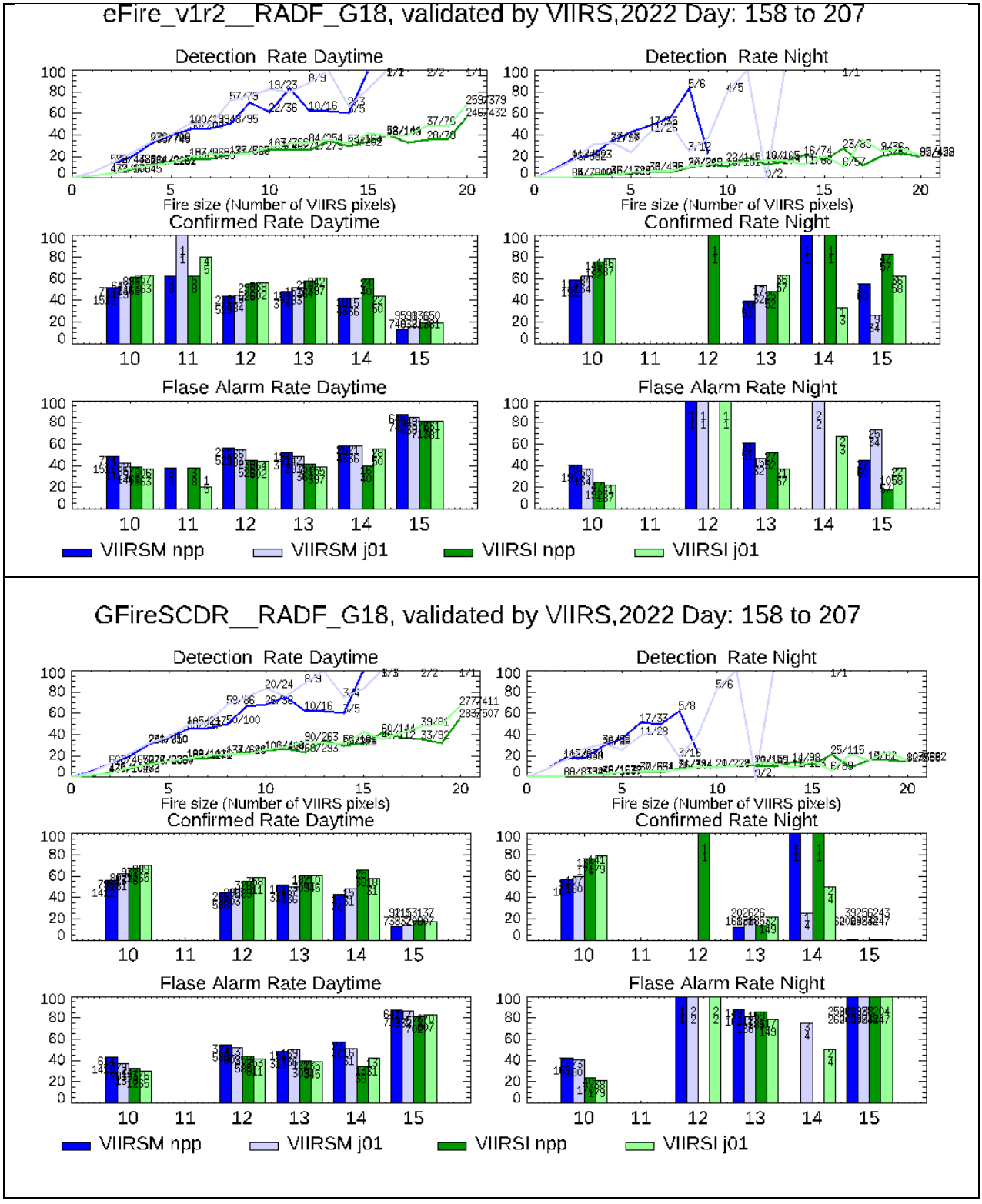

Figure 6-10 Comparing validation results of ABI G18 fire product derived by EFIRE (top) and WF_ABBA (OR files from SCDR, bottom) by VIIRS fire product using data DOY 158-207,2022

6.6 False alarms related to Sun glint pixels at edges of full disks of geostationary satellites

The sun glint related false alarms pixels were found in previous version ABI fire product (Fire products on SCDR). They are successfully removed from the EFIRE product.

Below are shown the number of fires detected by each ABI image when using WF_ABBA algorithm ("OR" fire product on SCDR) from day of year 158 to 207, 2022, for G16, G17, G18 respectively. For each satellite, huge number of fires were detected at specific hours only: For G16, this occurs near 4UTC and 7UTC; for G17 and G18, huge number of "fire" pixels (up to 9269 pixels for G17, 7583 pixels for G18) were found near 11UTC. Fires at those specific time are much more than the average number of fires detected by images at afternoon.

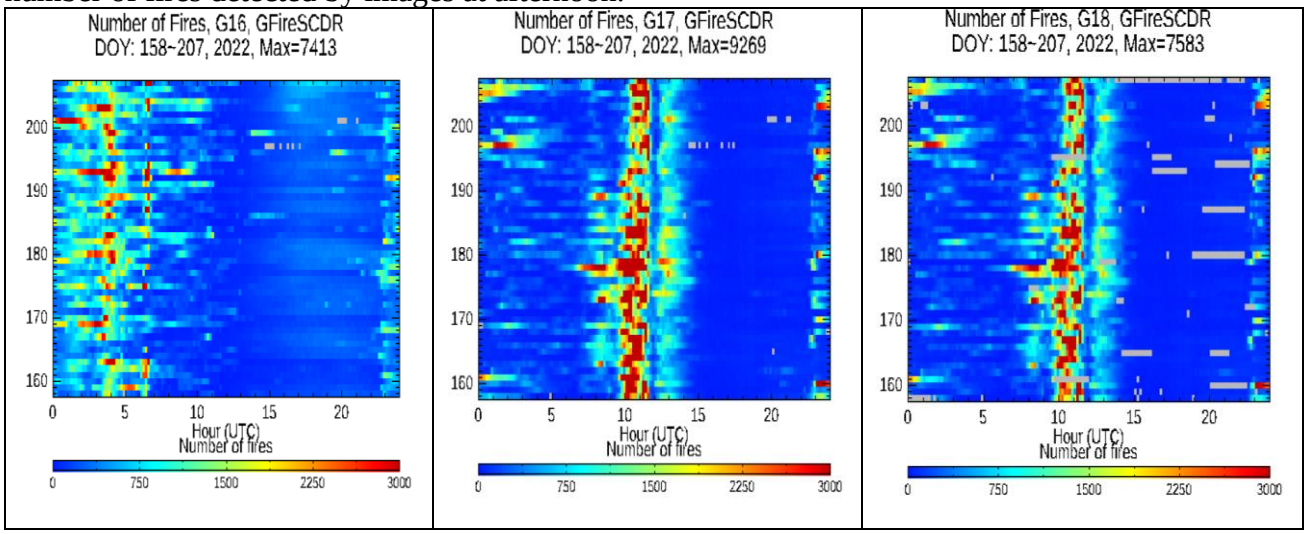

Figure 6-11 Number of fires detected on each ABI image (from DOY 158 to 207, 2022) for G16, G17, G18 respectively.

Figure 6-12 shows some examples of fire masks overlaid by fire pixels at the above specific time. These pixels are located at edge of full disk image, when the sun-pixel-satellite is almost on a straight line. Thus, they should be related to sun glint.

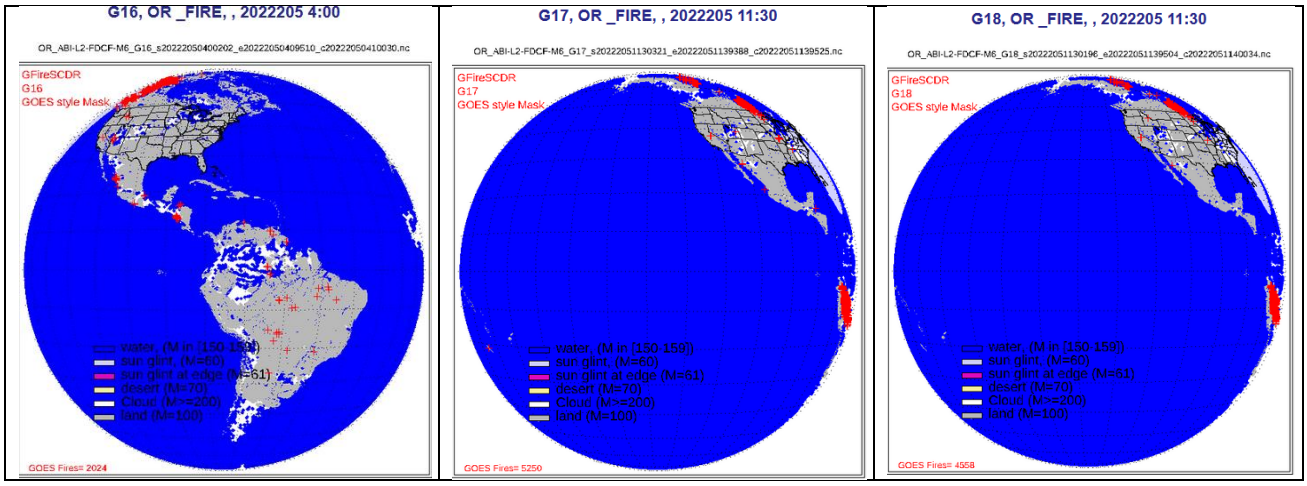

Figure 6-12 Examples of fire mask images overlaid by fire pixels generated from WF_ABBA algorithm. There are huge number of "fires" along the edge of full disk image.

By implementing a new test on sun glint near edge of full disk, EFIRE resolves this false alarm issue. Below are the number of fires detected by each ABI image by EFIRE algorithm (left panel), WF_ABBA algorithm (right panel, ABI fire product on SCDR). The color schemes were set as the same for both images. We can see the similar pattern except the above specific hours with sun glint issue.

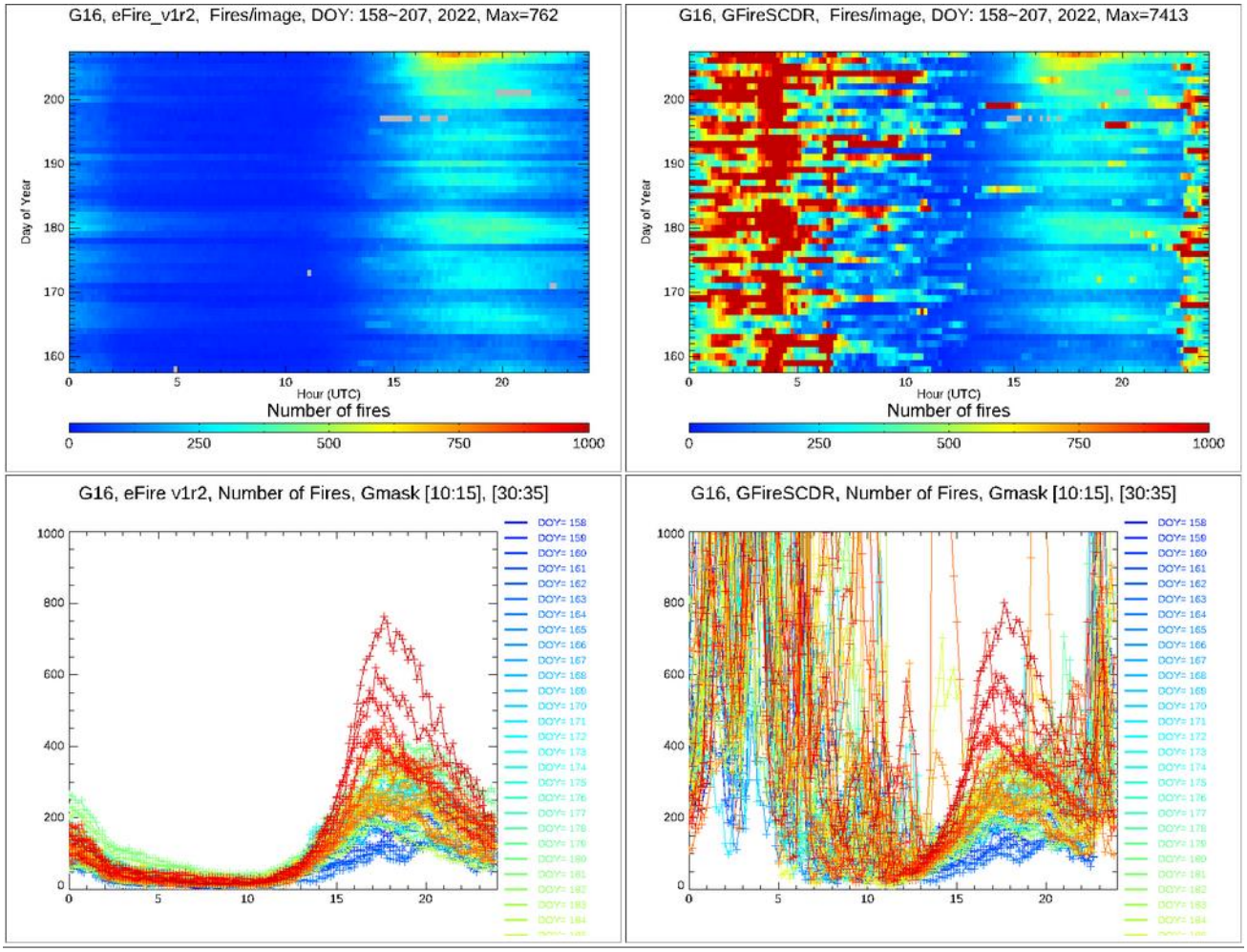

Figure 6-13 Comparison of the number of fires detected per G16 ABI image. Left: EFIRE, right: WF_ABBA.

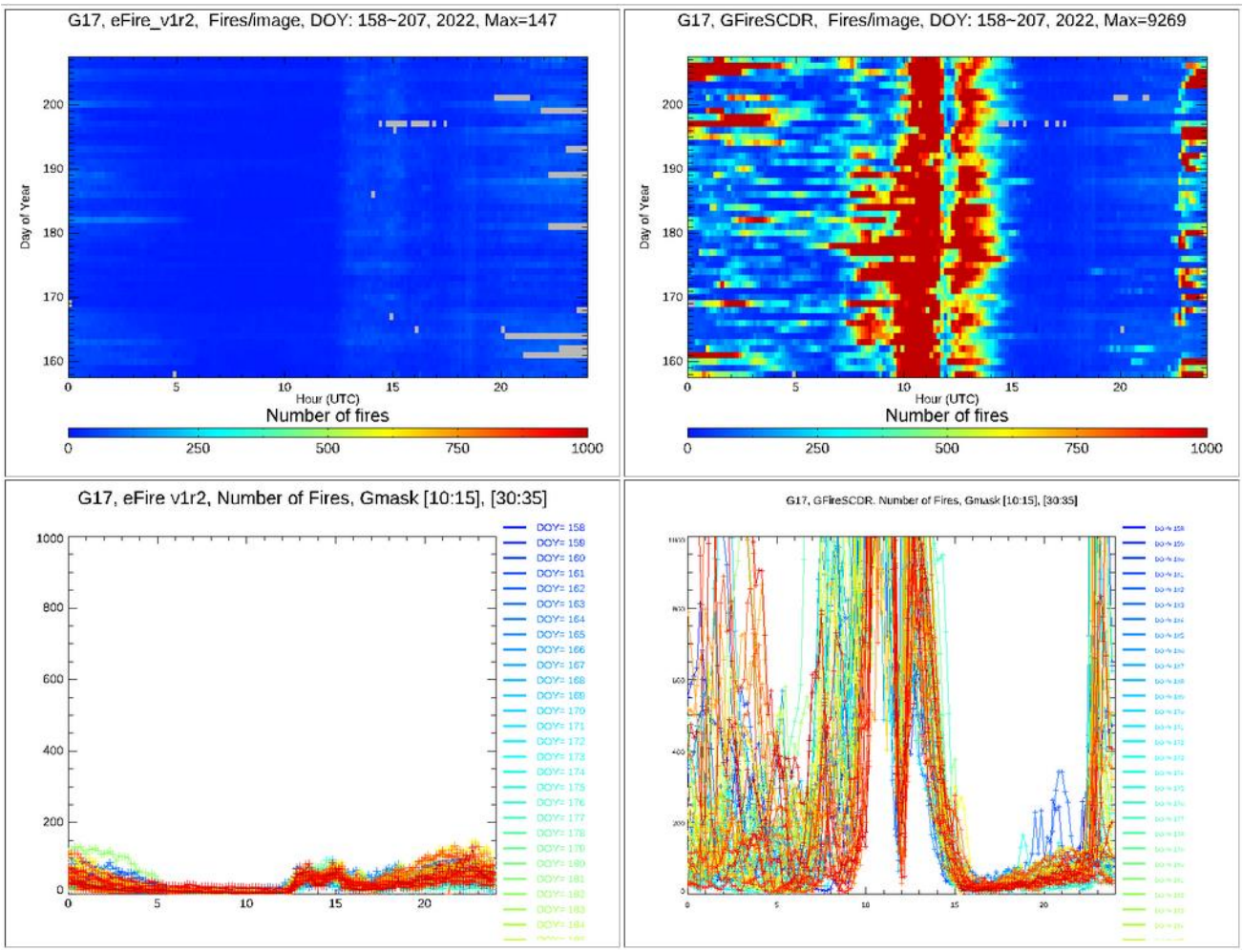

Figure 6-14 Comparison of the number of fires detected per G17 ABI image. Left: EFIRE, right: WF_ABBA.

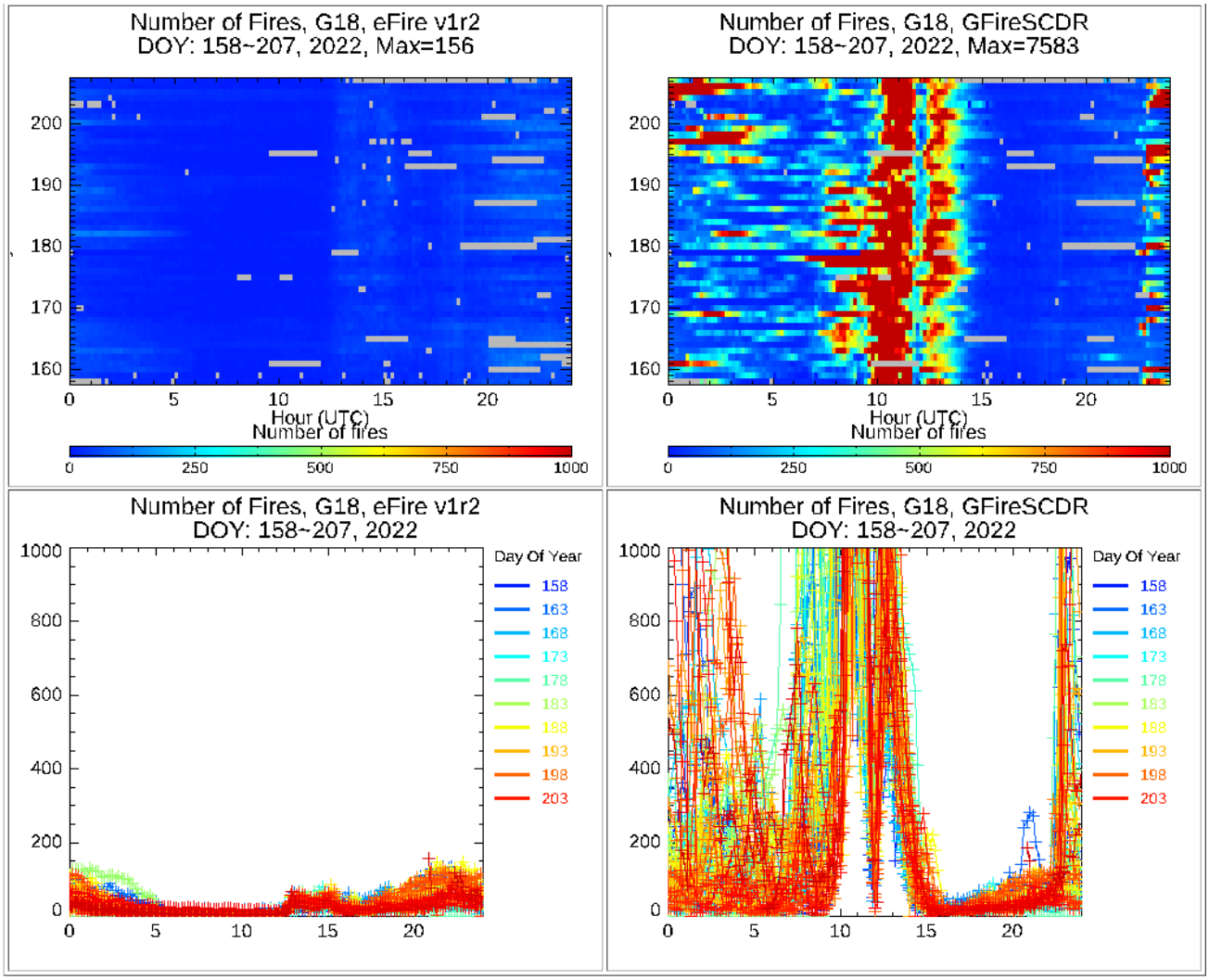

Figure 6-15 Comparison of the number of fires detected per G18 ABI image. Left: EFIRE, right: WF_ABBA.

When validating the ABI fire product by the VIIRS fire product, daily composite fire mask images of matched ABI-VIIRS pixels were created. Fire pixels of ABI and VIIRS pixels were overlaid on these images. Some obvious false alarm fire pxiels were found on image from WF_ABBA (left) because they neet the criteria of matching ABI and VIIRS pixles: time separation < 5 miniutes and VIIRS pixel falling into ABI fooot print defined by polygon of 4 corners of the pixel. This happens only at high latitude.
This was not shown in the image from EFIRE.

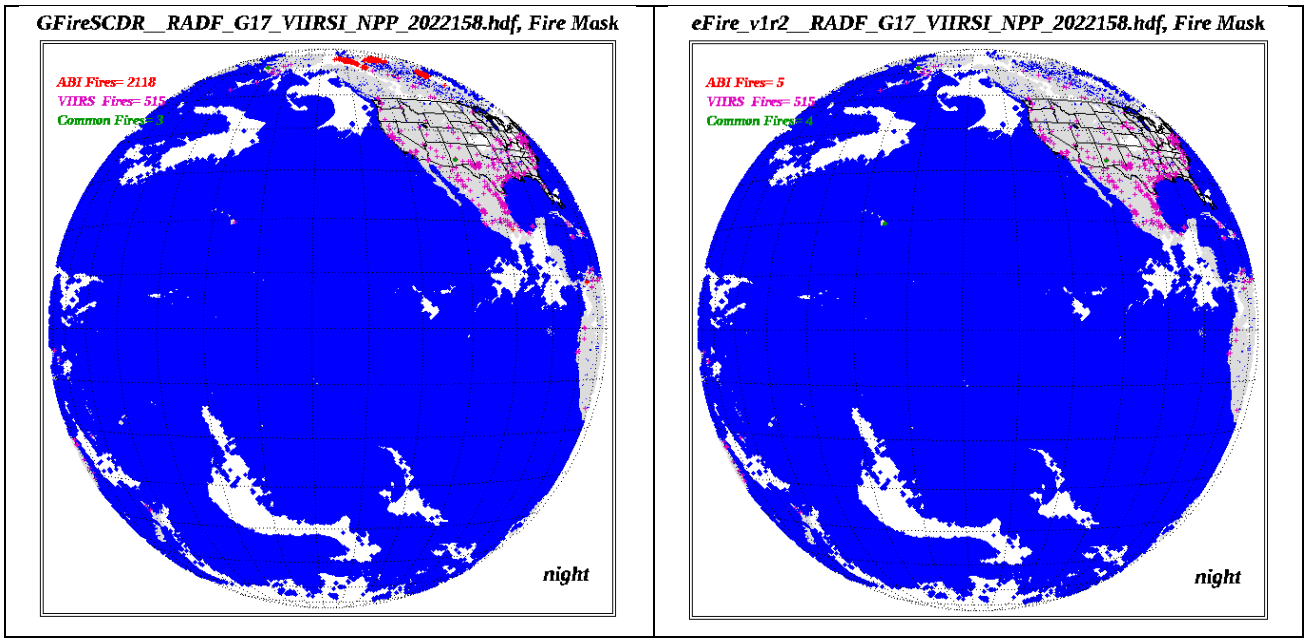

Figure 6-16 Daily composite Fire mask image of matched ABI-VIIRS pixels overlaid by fires. (left: from operation G17 product; right from EFIRE)

6.7 Consistency check between Fire Radiative Power (FRP) detected by various fire products.

So far, there are 10 fire products available for a given day.

- Daily fire product detected by SEVIRI (MSG2, MSG4), ABI (G16, G17, G18) produced by EFIRE system;
- Daily operational VIIRS fire product (NPP, J01, by using algorithm VIIRS-M and VIIRS-I) collected from STAR SCDR data library;
- MODIS fire product downloaded from NASA web site.

Here we present analysis of FRP retrievals June 19, 2022 (day of year 170).

Table 6-1Number of files of fire product available in June 19, 2022

sensor	satellite	Number of files
SEVIRI	MSG2	96
	MSG4	96
ABI	G16	144
	G17	144
	G18	142
VIIRS	VIIRS-M SNPP	1011
	VIIRS-I SNPP	1012
	VIIRS-M NOAA-20 (J01)	1013
	VIIRS-I NOAA-20 (J01)	1012
MODIS	Terra	288

FRP was generated for fire pixels and available in the above fire products. This allows us to compare the FRP generated by various sensor/satellite. Normalized histogram of FRP was calculated and illustrated as below. It shows the range of FRP values for each satellite. It was found that the distribution of FRP varies by sensor: the FRP plot of MG2 and MSG4 are similar, with peak value at 50, FRP of ABI (G16, G17, G18) has peak value at 20~30; FRP from VIIRS-M algorithm is very close to MODIS FRP (with peak value about 10); FRP from VIIRS-I algorithm is lower than others. As the distribution of FRP is related to size of pixel, this analysis confirms consistency among the FRP data from the various sensors.

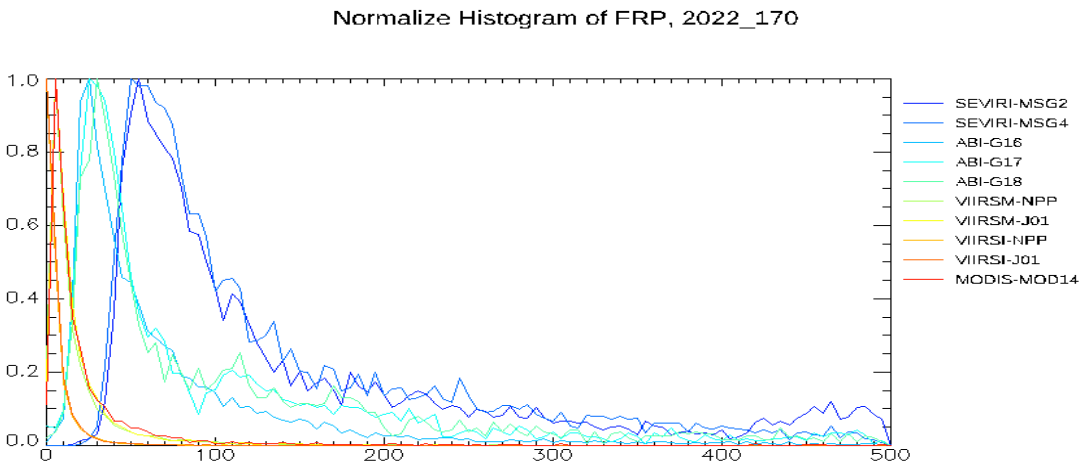

Figure 6-17 Normalized Histogram of FRP (statistics by using all images/granules of the given day, DOY 170,2022

7 Practical Considerations

Several issues involving numerical computation, programming and procedures, quality assessment and diagnostics, exception handling, and algorithm validation are considered in this section.

The fire algorithms utilize various static and dynamic ancillary input data sets as outlined in Section 3. The algorithm and code must be flexible enough to allow integration of modified/improved ancillary data sets as warranted through research and testing.

7.1 Numerical Computation Considerations

The fire algorithms are based on a decision tree approach and only requires numerical methods for determining sub-pixel fire characteristics for a small subset of the total number of pixels in an image. The algorithm performs operations that require accurate conversion from temperature to channel radiance and channel radiance to temperature.

7.2 Programming and Procedural Considerations

Although possible fires are determined on a pixel by pixel basis, the fire algorithm requires an expanding window around the pixel being evaluated to determine the background conditions for the visible, 3.9 µm and 11 µm channels. Fire pixel determination involves a series of decision trees. This allows identification of all possible fire pixels (step 1) and further refinement of the product (step 2). Fire confidence categories and flags are used to provide the end user fire characterization and not just fire location information.

7.3 Quality Assessment and Diagnostics

The output fire mask includes fire confidence information and meta data regarding processing issues and block-out zones (such as Sun glint, high satellite zenith, missing data, bad data etc.). Future calibration and validation will be based on comparison of the ABI /SEVIRI fire product with high resolution data (e.g. 30 m Landsat 8 or 9 ETM+, Terra ASTER, Landsat Data Continuity Mission OLI - launch 2011) which is performed on a routine basis.

Statistics summarizing ongoing inter-comparisons of ABI/SEVIRI and VIIRS fire products were generated and evaluated.

7.4 Exception Handling

Most run-time exceptions are handled by the framework running the fire code. Pixel level exception will be recorded in quality flags in fire product.

8 Validating EFIRE ABI and SEVIRI fire by Landsat fire product

Landsat data has high resolution (30 meters) compared to ABI and SEVIRI, and with observations at very low satellite zenith angle (near nadir). It is a nice data base to validate ABI or SEVIRI EFIRE product although Landsat data is only available at local time of 10 a.m.: *Landsat 8* and Landsat 9 *cross* the *equator* at 10:00 a.m. +/- 15 minutes (mean local *time*) in their respective orbits.

8.1 The procedure of validating ABI /SEVIRI fire product by Landsat fire product

A procedure for validating fire products from geostationary satellites (ABI/SEVIRI) by Landsat fire product were developed. It includes:

- Download collection 2 Landsat reflectance (Landsat 8 and 9, band 1-7) from USGS,
- Generate Landsat fire product by using algorithm (Schroeder et al., 2016) and code developed by Wilfrid Schroeder (NOAA/NESDIS/OSPO);
- Run daily matching procedure to find out the time and spatial matched pairs of "ABI (SEVIRI) vs Landsat" cloud free pixels (fire or land pixels). Details are described on the flowchart below.
- Generate multiple days' summary validation report from daily records.

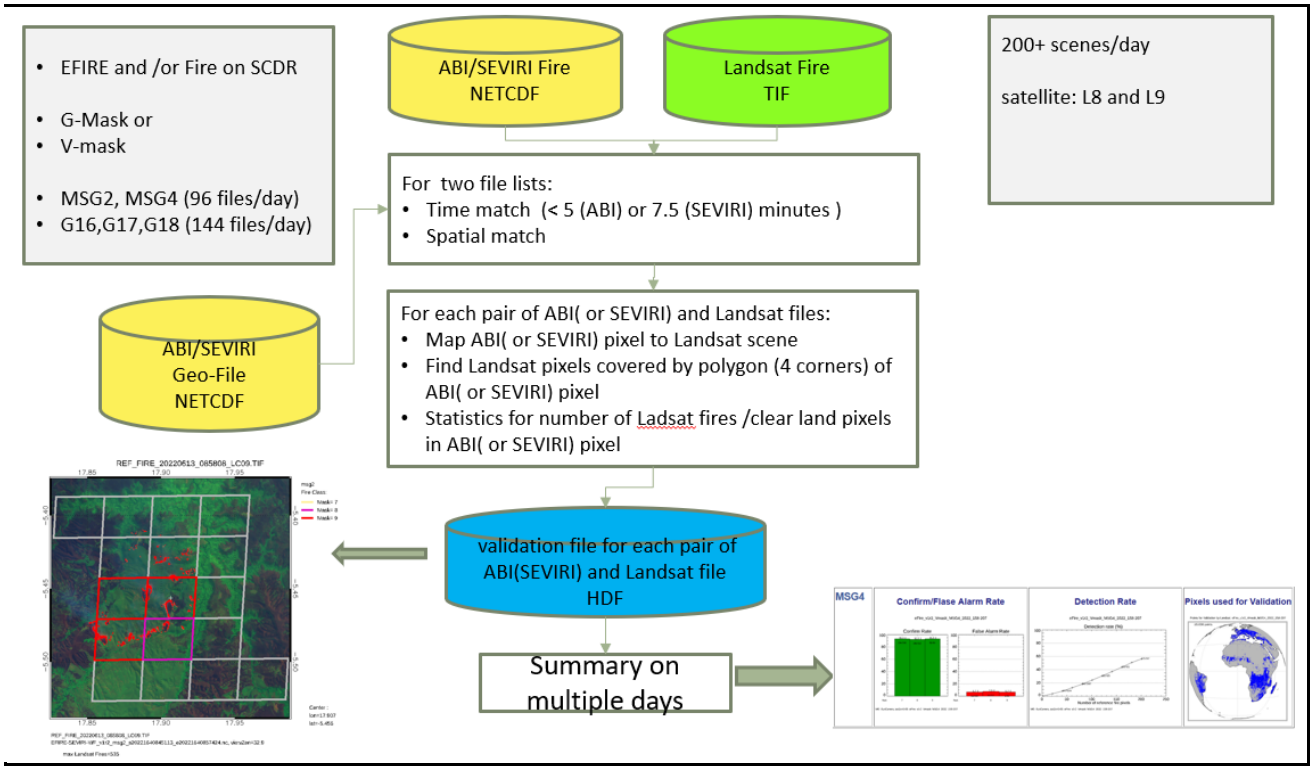

Figure 8-1 Flow chart of Validation module for validating fire product derived from geostationary satellites (ABI/SEVIRI) by high resolution (30m) Landsat data.

8.2 Collecting Landsat data

Landsat scenes were labeled and organized by path/row number. Each scene is located at specific location (with specific latitude and longitude range). If a Landsat scene is over land (determined by 1km Land sea mask) and within the domain of given geostationary satellite, then this Landsat scene was selected to download and saved in unique scene list for given satellite. In order to validate multiple satellites (ABI: G16, G17, G18, SEVIRI: MSG1, MSG2, MSG4), we merged the unique scene lists together.

The figure below shows the location of selected Landsat scenes (defined by path/row numbers) which are collected routinely. They are good for validating fire products detected by ABI and SEVIRI satellites.

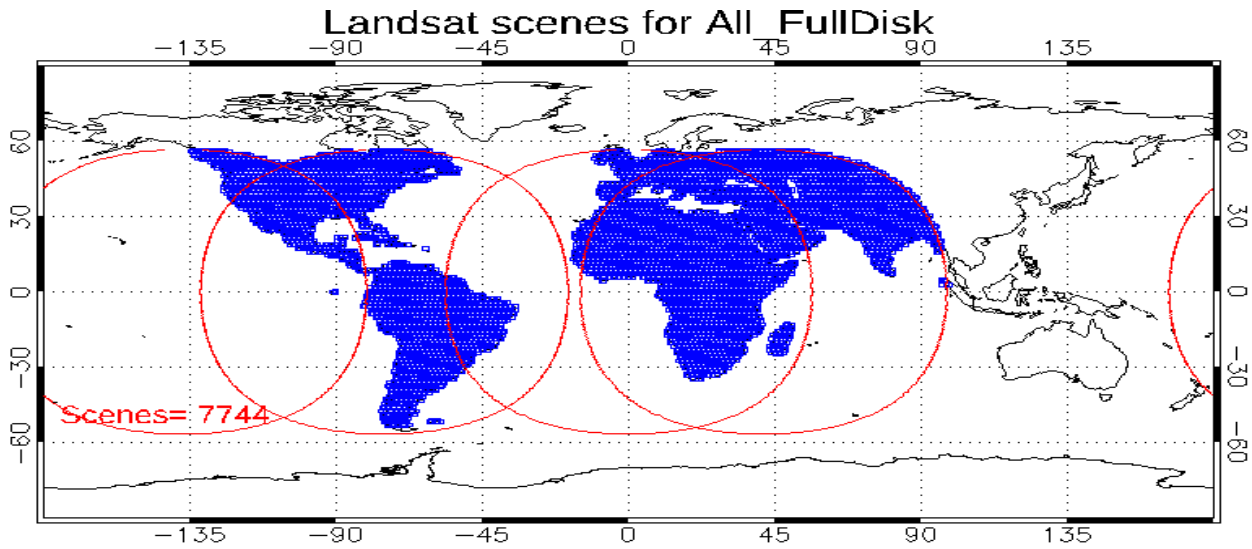

Figure 8-2 Landsat scenes collected for validating fire product derived from geostationary satellites (ABI/SEVIRI)

The available Landsat scenes can be found it the meta data file for Landsat 8 and 9 on USGS web site. https://landsat.usgs.gov/landsat/metadata_service/bulk_metadata_files/
LANDSAT_OT_C2_L1.csv.gz.

Only scenes with cloud amount <20% and in the above pre-selected list will be download. Starting from January 2022, both Landsat 8 and 9 are available. The figure below shows the location of Landsat scenes downloaded during the 3 days (day 157 to 159, 2022).

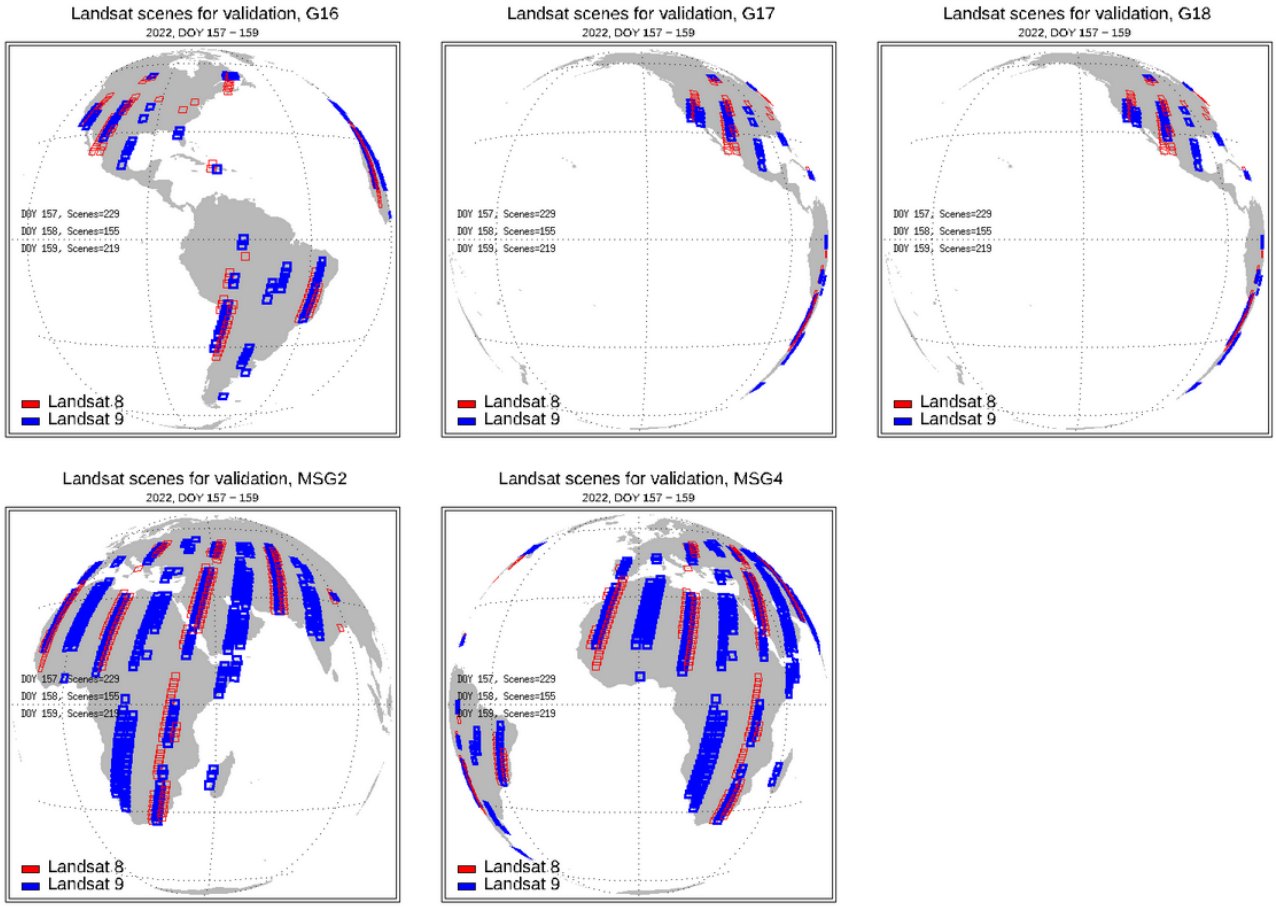

Figure 8-3The Landsat scenes downloaded during the daytime periods of days 157-159, 2022).

When downloading a Landsat scene, reflectance of band 1-7 (B*.TIF), quality flags file (*QA*.TIF) angle (ANG.txt) files, metadata (MTL.txt) were downloaded. Then, Landsat fire product (*.TIF) is created by using Wilfrid Schroeder's fire detection code for Landsat. Reflectance images of band 7,5,2 are saved in separate HDF file if this scene contain "big fire" (the number of Landsat pixels in an ABI/SEVIRI pixel > 20). They are used to generate Landsat RGB images overlaid by ABI /SEVIRI pixels.

8.3 Matched ABI/SEVIRI-Landsat pixels used for validation

The actual Landsat scenes used for validating G18 fire product for the period 158 to 207, 2022 were shown as below. Only the data pairs with satellite zenith angle <65 degree were used for validation.

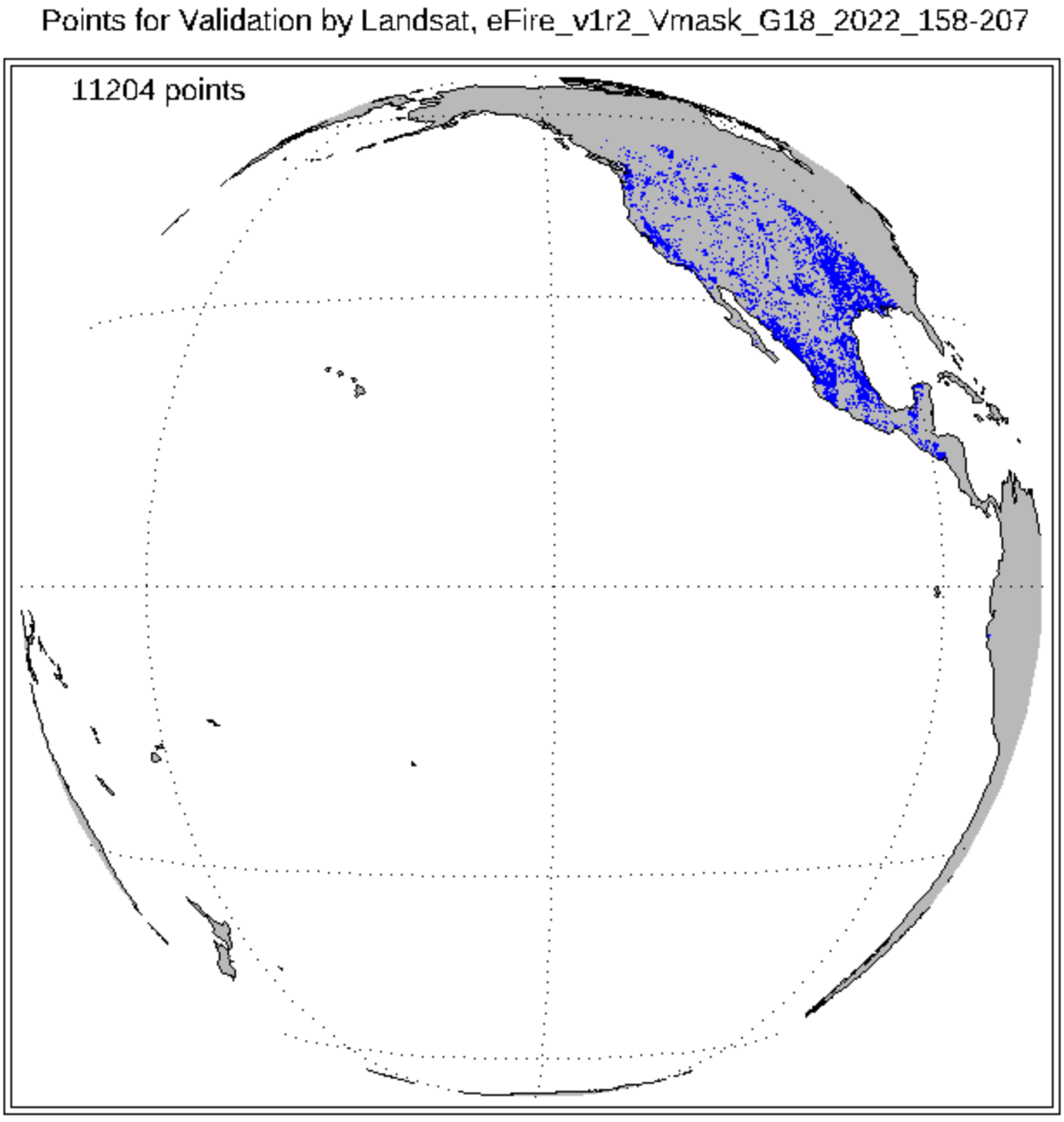

Figure 8-4 Location of Landsat scenes used for validating G18 ABI, from DOY 158 to 192, 2022

8.4 Landsat images overlaid by ABI / SEVIRI fire pixels

Examples of Landsat images (RGB composite using Land sate band 7,5,2) overlaid by ABI / SEVIRI fire pixels were created for big fires. Below are selected cases of ABI / SEVIRI fires confirmed by Landsat fire product. There are also false alarm cases (not shown).

Comparison between these images and google map shows Landsat data were processed correctly in terms of geolocation.

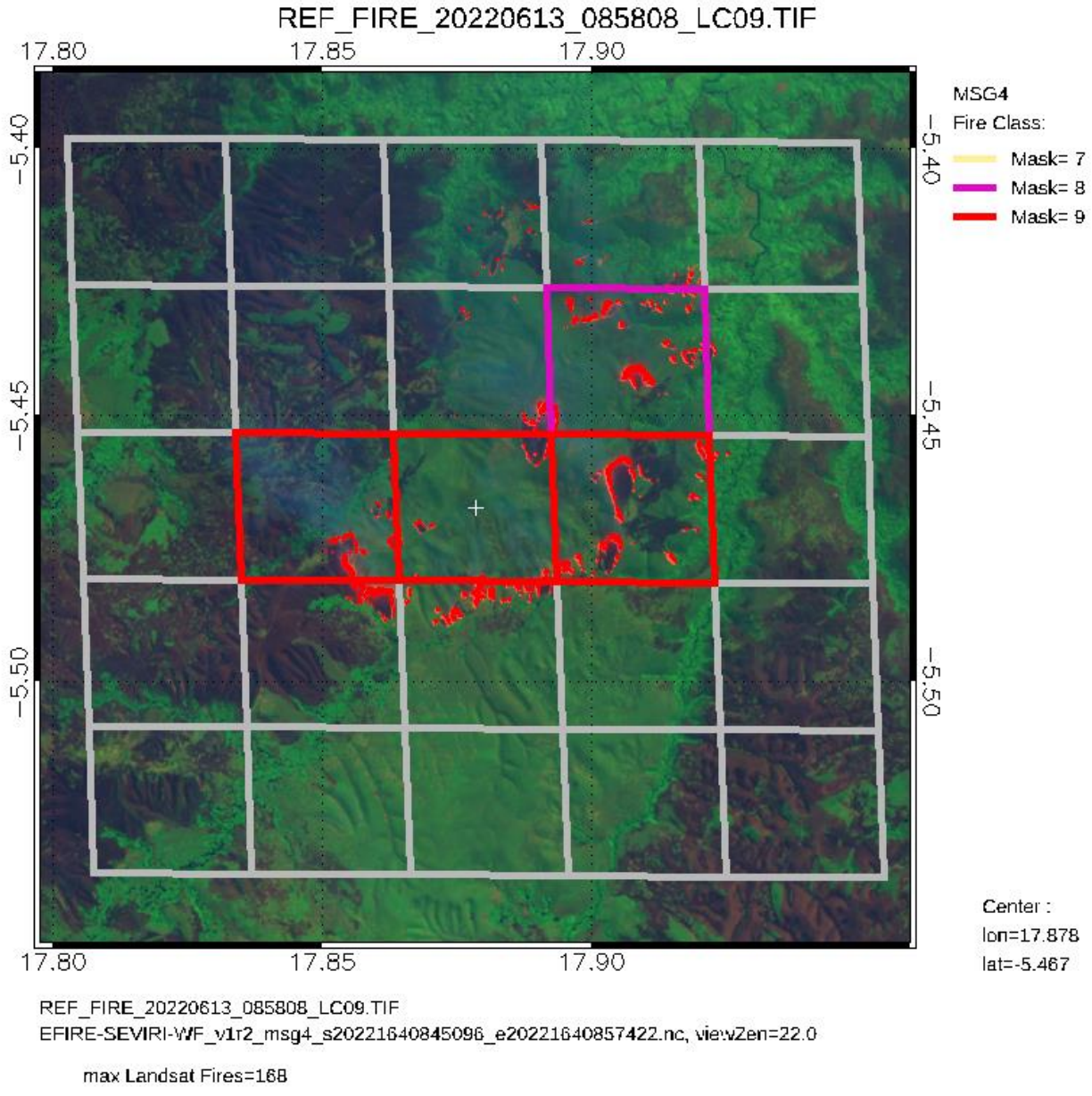

Figure 8-5 Landsat RGB image (channel 7,5,2) overlaid by MSG4 SEVIRI pixels (thick grid, colored by fire classes).

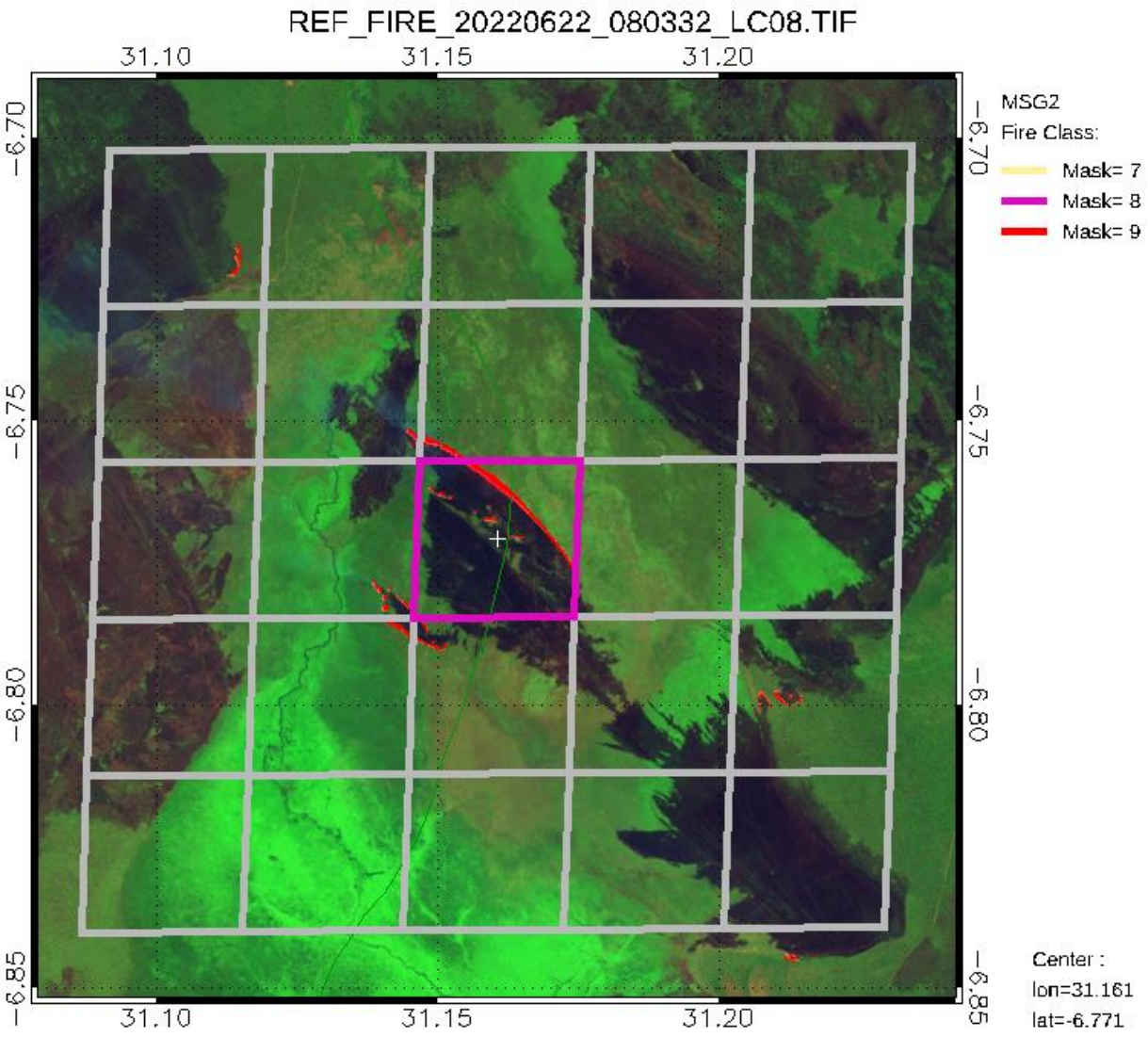

Figure 8-6 Landsat RGB image (channel 7,5,2) overlaid by MSG2 SEVIRI pixels (thick grid, colored by fire classes).

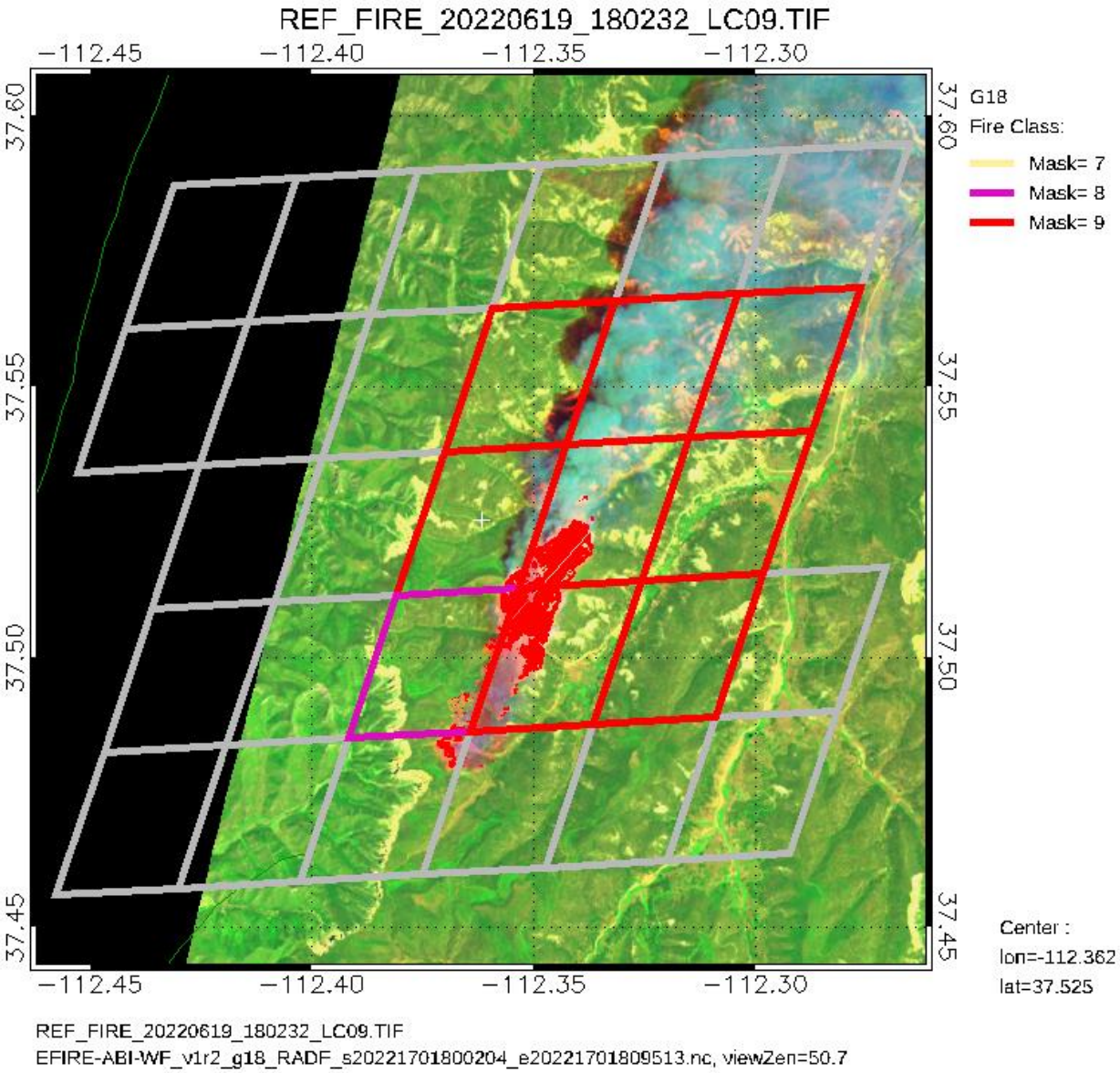

Figure 8-7 Landsat RGB image (channel 7,5,2) overlaid by G18 ABI pixels (thick grid, colored by fire classes).

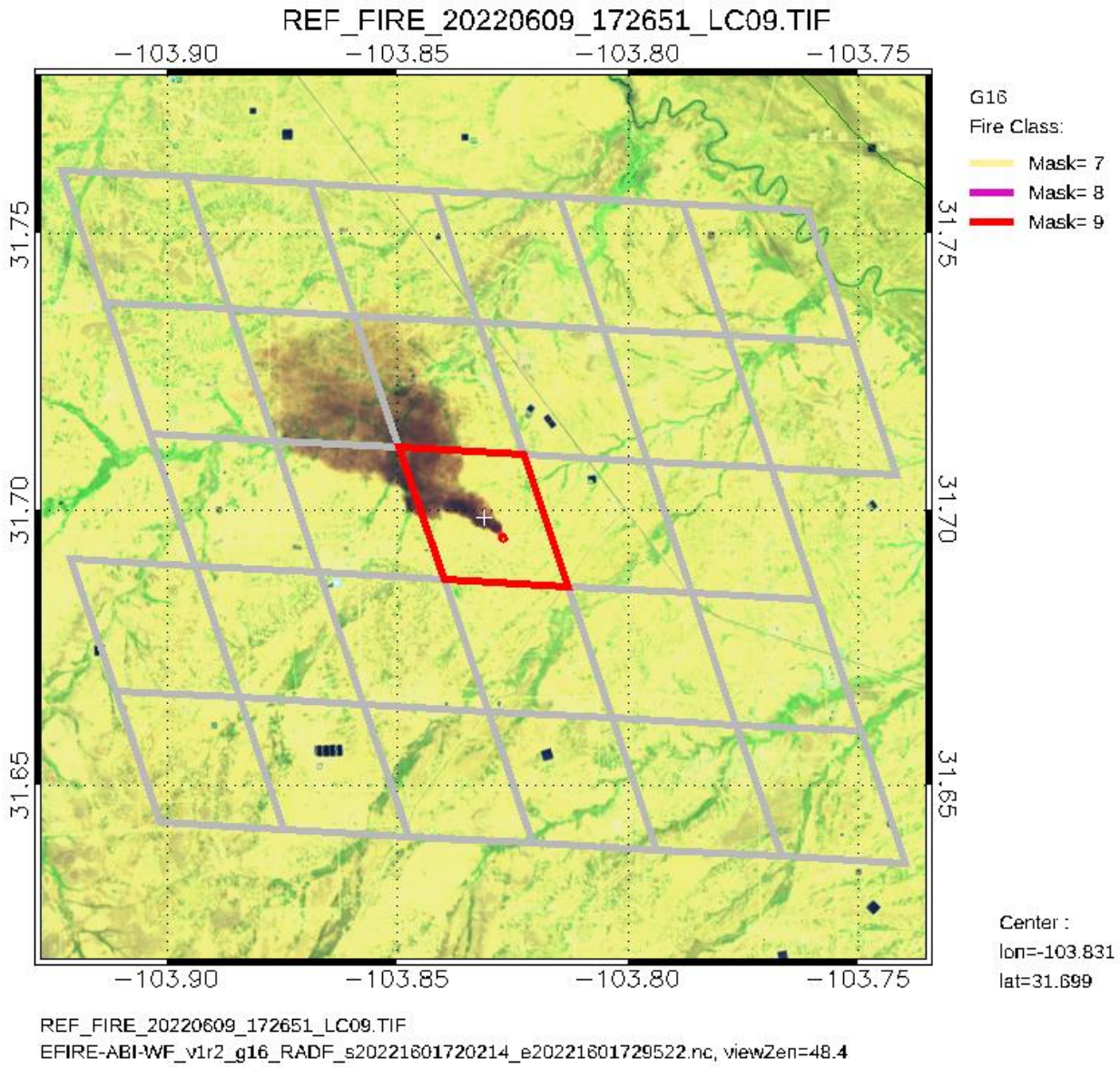

Figure 8-8 Landsat RGB image (channel 7,5,2) overlaid by G16 ABI pixels (thick grid, colored by fire classes).

8.5 Validating SEVIRI fire product by Landsat fire product.

EFIRE products from SEVIRI (MSG2 and MSG4) was validated by using Landsat fire product for the period of day 158-207, 2022. The result shows very good confirm rate (>81%) for all 3 fire classes (low, medium and high confidence)

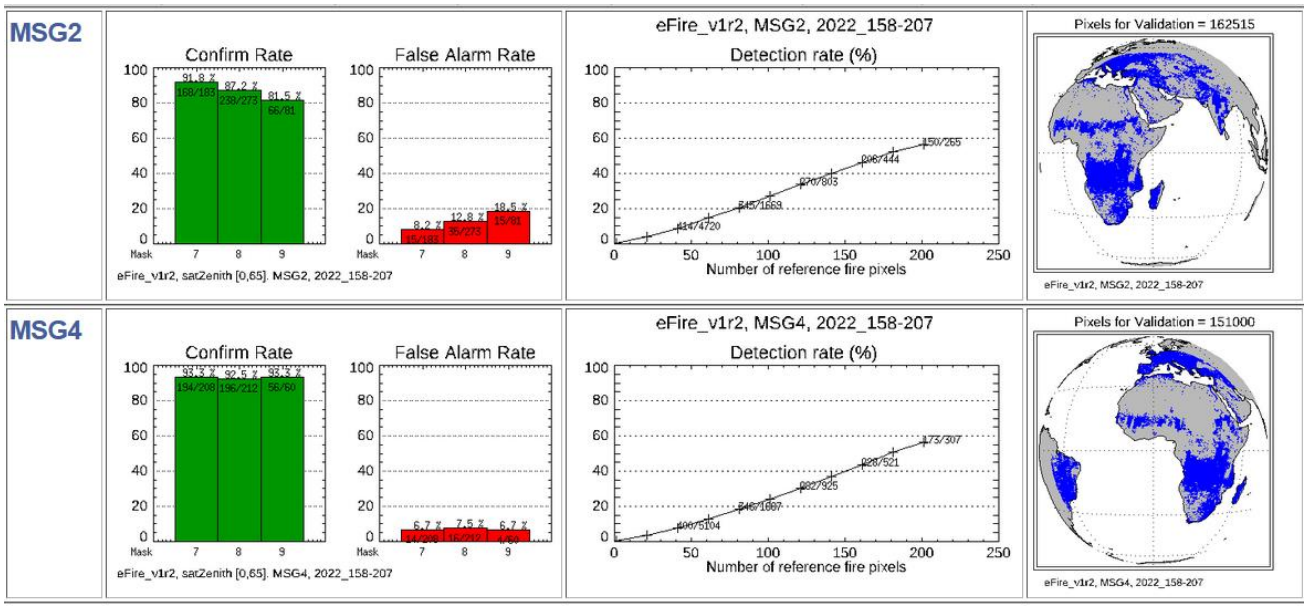

Figure 8-9 Result of validating SEVIRI fire by Landsat fire product

```
Result of Validating MSG4 fire product by Landsat fire product:
eFire_v1r2, MSG4, 2022_158-207
Using MSG4 data with satellite zenith in [ 0, 65]

 --------------  confirm_rate_by_class --------------
Fire Mask Class          =     7,    8,    9
MSG4 fire Pixels         =   208,  212,   60
Confirmed fires          =   194,  196,   56
False alarm points       =    14,   16,    4
Confirmed rate (%)       =  93.3, 92.5, 93.3
False alarm rate (%)     =   6.7,  7.5,  6.7

--------------  detection_rate_overall --------------
 Detection_rate if number of Landsat fires in a MSG4 foot print > threshold
 Reference Pixels =    1,   21,   41,   61,   81,  101,  121,  141,  161,  181,  201
 Detection Rate(%)=  0.3,  3.6,  7.8, 13.0, 18.3, 24.2, 30.5, 37.0, 43.8, 50.9, 56.4
```

8.6 Validating ABI fire by Landsat fire product.

EFIRE products from ABI (G16, G17, G18) was validated by using Landsat fire product for the period of day 158-207, 2022. The result shows 91% of fires with high confidence was confirmed by Landsat fire detection, 83% and 71% for medium and low confidence fire.

Both G17 and G18 were located at the same longitude (-137.2) during the validation period. The validation scores for G17 and G18 are similar, in both cases, the confirmed rate is much lower than G16. This may be due to the large satellite zenith of the available validation samples.

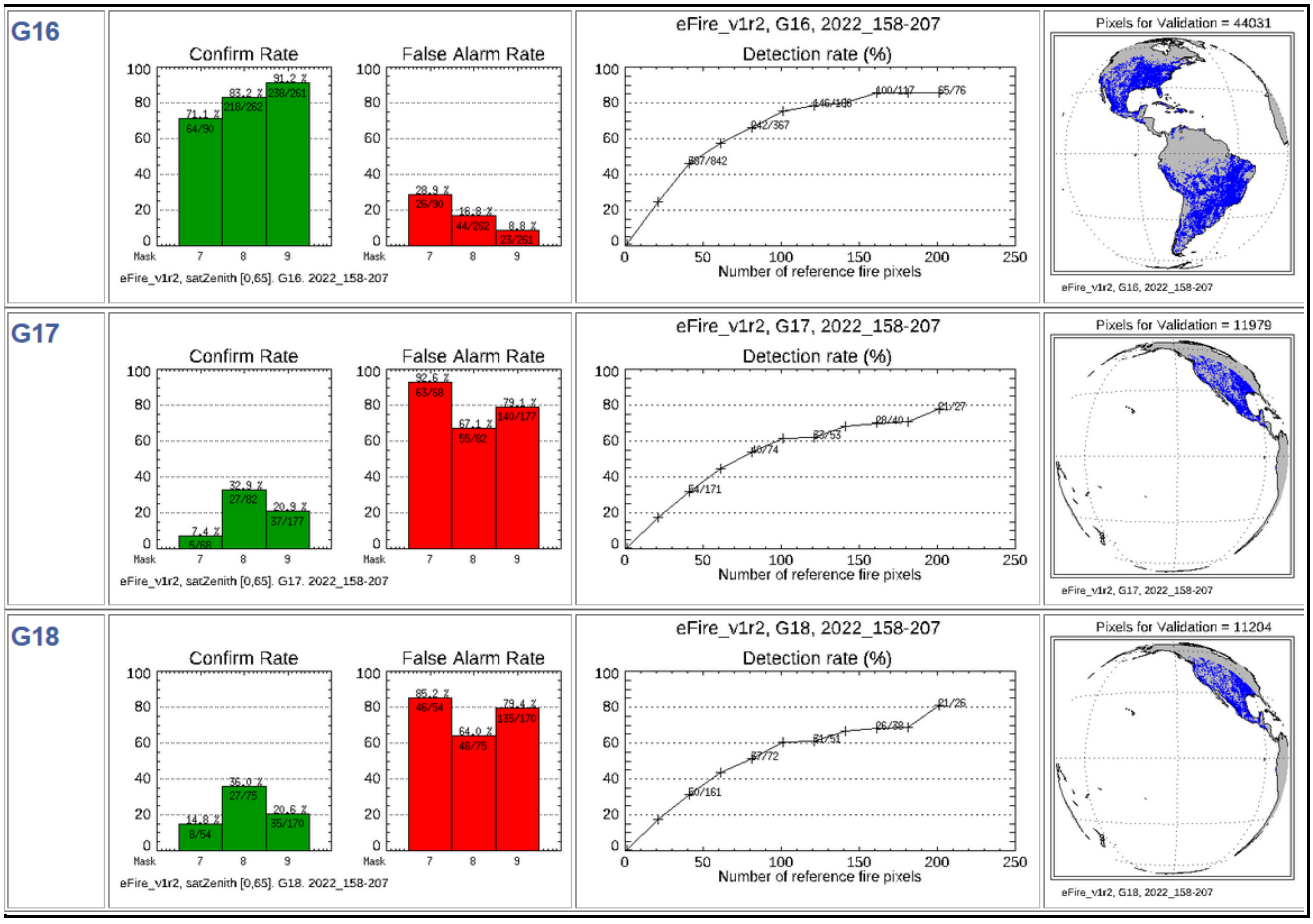

Figure 8-10 Result of validating ABI (G16, G17, G18) fire by Landsat fire product

8.7 Comparing validation result on ABI fire: EFIRE vs. current fire product

Two versions of ABI fire products (EFIRE and current ABI fire product) observed by satellite G16, G17, G18 were validated by using Landsat fire product for the period of day 158-207, 2022. Since the current baseline fire product only contains the GOES style fire mask ("Gmask") array (with 12 fire classes), the validation results were evaluated by using the similar GOES style fire mask in EFIRE. The validation scores were shown by statistics on 6 fire classes (after merged the time filtered fire classes with normal fire classes).

The validation result on EFIRE and current fire product are very close, because the major improvement in EFIRE is on removing the false alarms related to the "sun glint near full disk edge", which does not occur at the time when matched ABI – Landsat pixels were found (near 10:00AM local time).

G16, eFire_v1r2

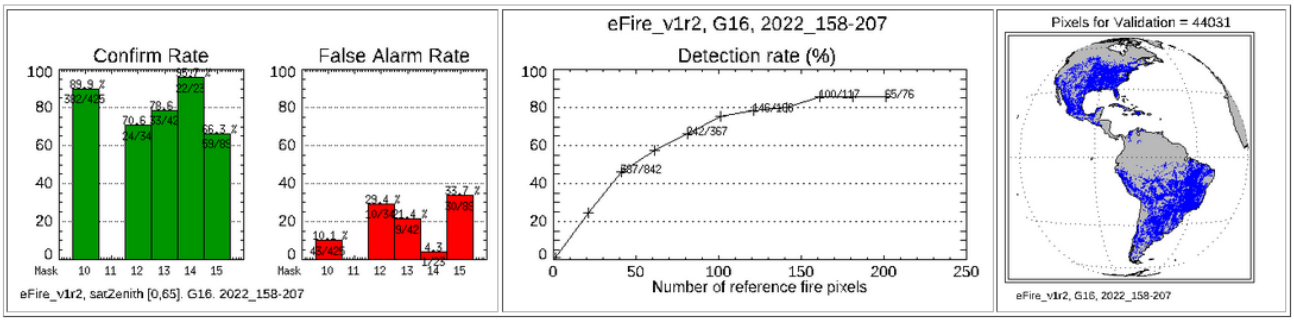

G16, GFireSCDR

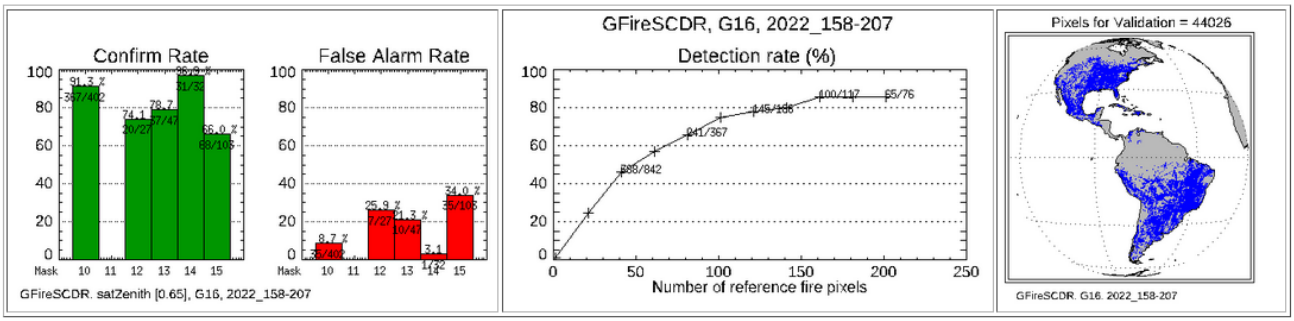

Figure 8-11 Result of validating G16 ABI fire by Landsat fire product, comparing between EFIRE (top) and current ABI product (bottom, fire product on SCDR)

G17, eFire_v1r2

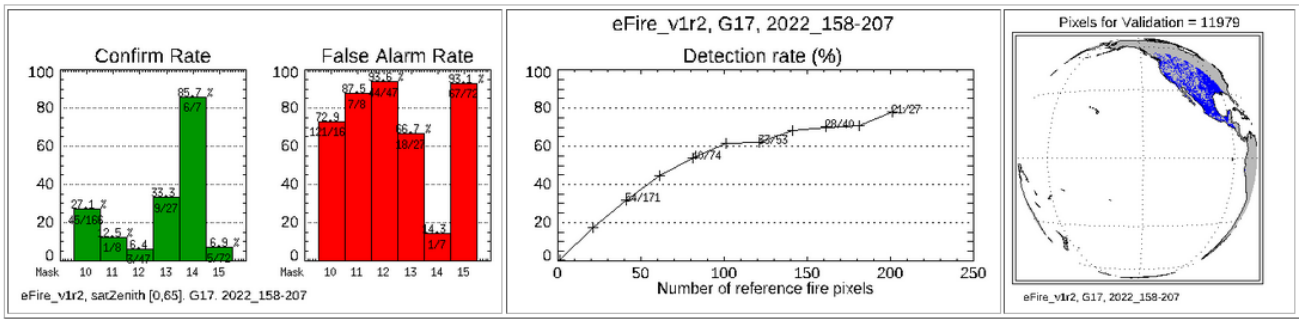

G17, GFireSCDR

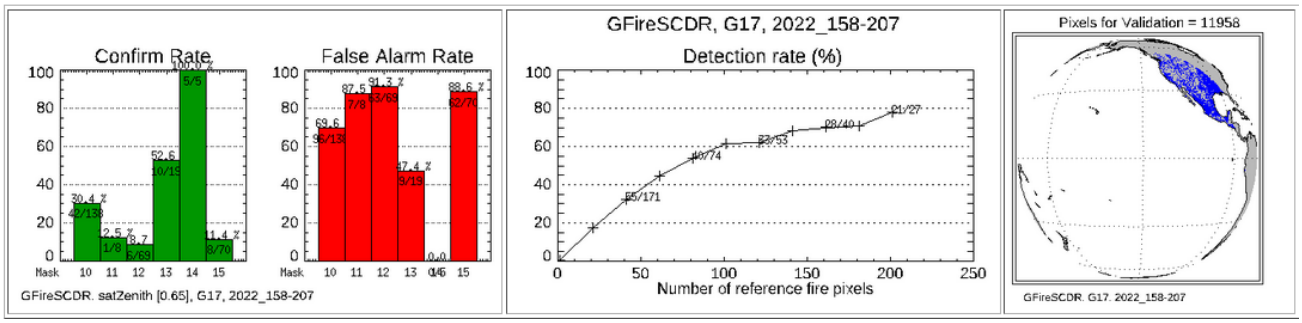

Figure 8-12 Result of validating G17 ABI fire by Landsat fire product, comparing between EFIRE (top) and current ABI product (bottom, fire product on SCDR)

G18, eFire_v1r2

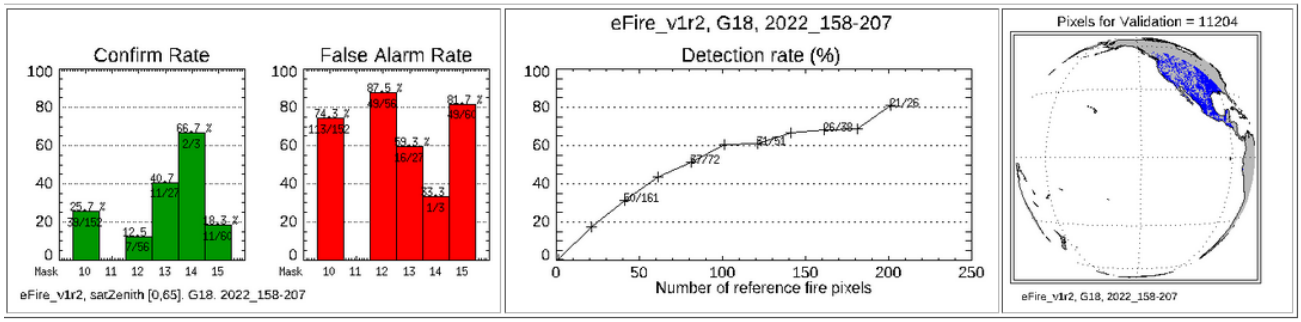

G18, GFireSCDR

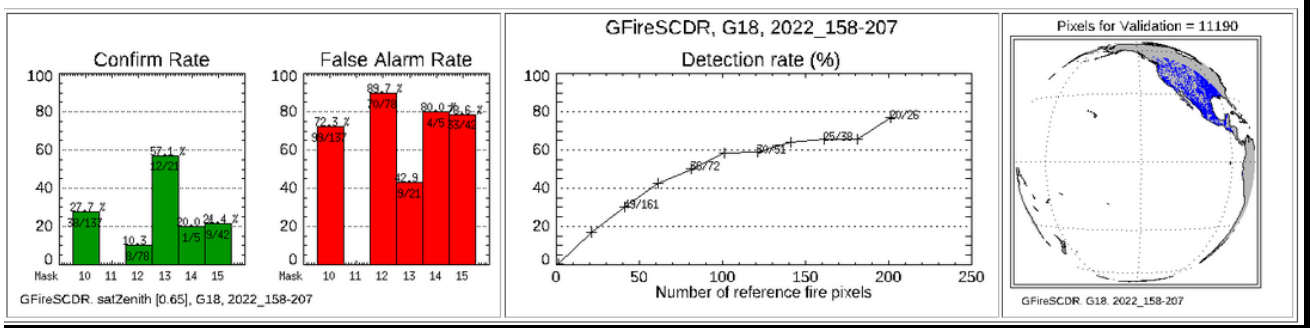

Figure 8-13 Result of validating G18 ABI fire by Landsat fire product, comparing between EFIRE (top) and current ABI product (bottom, fire product on SCDR)

9 Assumptions and Limitations

The assumptions made and potential limitations concerning the algorithm theoretical basis and performance are described in this section.

Several assumptions have been made concerning performance estimates. Most of the limitations cited in this section are common to all current and proposed environmental monitoring instruments on weather satellites.

9.1 limitations

The algorithm is limited by the availability of accurate input data. It is assumed that the input test data is representative of what the post-launch data will look like, however unforeseen differences could impact performance.
Specific limitations are listed as follows:

- Missing required bands (band 4μm and 11μm), The algorithm will fail and cannot proceed.

- Missing TPW data from an NWP model. The algorithm process with option of water vapor correction, it will process fire product without water vapor data (water vapor affects fire temperature retrieval only).

- Missing ancillary data. All ancillary data are provided by "EFIRE parameter file"; EFIRE will fail without this file.

9.2 EFIRE Performance

The EFIRE algorithm performance assumptions are as follows. It has been tested on Linux system with 8GB RAM and at least 100GB free disk. The code is written and compiled as a single-threaded application. Performance is proportional to the number of detected fires. High fire activity or high levels of noise that appear to be associated with high fire activity can increase runtime.

Table 9-1 Resource used by EFIRE system

	RAM GB	Minutes for Processing one image
ABI (Full Disk)	2.9	1.0
SEVIRI (Full Disk)	1.4	0.5
VIIRS (granule)	0.5	0.3
VII (granule)	0.5	0.3

References

Louis Giglio, Wilfrid, Ivan Csiszar, Marina Tsidulko, 2020: **VIIRS Active fire algorithm theoretical basis document** Version 2.8, (VIIRS-M band fire detection algorithm, Algorithm_Theoretical_Basis_Document_NDEAF_2.8_012820.docx).

Christopher C. Schmidt, Elaine Prins, Scott Lindstrom, 2020, **GOES-R Advanced Baseline Imager (ABI) Algorithm Theoretical Basis Document For Fire / Hot Spot Characterization,** Version 2.7. https://www.star.nesdis.noaa.gov/goesr/rework/documents/ATBDs/Enterprise/GOES-R_AWG_ATBD_Land_FIRE_v2.7_Oct2020.pdf

Wilfrid Schroeder, Louis Giglio, Ivan Csiszar, Marina Tsidulko, 2020, **Algorithm Theoretical Basis Document for NOAA NDE VIIRS I-band (375m) Active Fire** (ATBD_Iband_ActivEFIREs_v1.0_2020_June.pdf) https://www.star.nesdis.noaa.gov/jpss/documents/ATBD/ATBD_Iband_ActiveFires_v1.0.pdf

Wilfrid Schroeder, Patricia Oliva, Louis Giglio, Brad Quayle, Eckehard Lorenz, Fabiano Morelli, 2016, **Active fire detection using Landsat-8/OLI data**, Remote Sensing of Environment 185 (2016) 210–220

Giglio, L., Descloitres, J., Justice, C. O., Kaufman, Y. J. (2003). An enhanced contextual fire detection algorithm for MODIS. *Remote Sensing of Environment,* 87, 273–282.

END OF DOCUMENT